Catestatin Gly364Ser Variant Alters Systemic Blood Pressure and the Risk for Hypertension in Human Populations via Endothelial Nitric Oxide Pathway

Malapaka Kiranmayi, Venkat R. Chirasani, Prasanna K.R. Allu, Lakshmi Subramanian, Elizabeth E. Martelli, Bhavani S. Sahu, Durairajpandian Vishnuprabu, Rathnakumar Kumaragurubaran, Saurabh Sharma, Dhanasekaran Bodhini, Madhulika Dixit, Arasambattu K. Munirajan, Madhu Khullar, Venkatesan Radha, Viswanathan Mohan, Ajit S. Mullasari, Sathyamangla V. Naga Prasad, Sanjib Senapati, Nitish R. Mahapatra

Abstract—Catestatin (CST), an endogenous antihypertensive/antiadrenergic peptide, is a novel regulator of cardiovascular physiology. Here, we report case–control studies in 2 geographically/ethnically distinct Indian populations (n≈4000) that showed association of the naturally-occurring human CST-Gly364Ser variant with increased risk for hypertension (age-adjusted odds ratios: 1.483; *P*=0.009 and 2.951; *P*=0.005). Consistently, 364Ser allele carriers displayed elevated systolic (up to ≈8 mm Hg; *P*=0.004) and diastolic (up to ≈6 mm Hg; *P*=0.001) blood pressure. The variant allele was also found to be in linkage disequilibrium with other functional single-nucleotide polymorphisms in the *CHGA* promoter and nearby coding region. Functional characterization of the Gly364Ser variant was performed using cellular/molecular biological experiments (viz peptide–receptor binding assays, nitric oxide [NO], phosphorylated extracellular regulated kinase, and phosphorylated endothelial NO synthase estimations) and computational approaches (molecular dynamics simulations for structural analysis of wild-type [CST-WT] and variant [CST-364Ser] peptides and docking of peptide/ligand with β-adrenergic receptors [ADRB1/2]). CST-WT and CST-364Ser peptides differed profoundly in their secondary structures and showed differential interactions with ADRB2; although CST-WT displaced the ligand bound to ADRB2, CST-364Ser failed to do the same. Furthermore, CST-WT significantly inhibited ADRB2-stimulated extracellular regulated kinase activation, suggesting an antagonistic role towards ADRB2 unlike CST-364Ser. Consequently, CST-WT was more potent in NO production in human umbilical vein endothelial cells as compared with CST-364Ser. This NO-producing ability of CST-WT was abrogated by ADRB2 antagonist ICI 118551. In conclusion, CST-364Ser allele enhanced the risk for hypertension in human populations, possibly via diminished endothelial NO production because of altered interactions of CST-364Ser peptide with ADRB2 as compared with CST-WT. **(*Hypertension*. 2016;68:334-347. DOI: 10.1161/HYPERTENSIONAHA.116.06568.)** ● **Online Data Supplement**

Key Words: chromogranin A ■ genetic association study ■ genetic variation ■ hypertension ■ nitric oxide

Chromogranin A (CHGA) is a ≈50-kDa soluble, acidic glycoprotein that plays an essential role in the formation of catecholamine secretory vesicles in neuronal, endocrine, and neuroendocrine tissues.[1] Expression levels of *CHGA* have been found to be elevated in rodent models of both genetic[2] and acquired forms of hypertension.[3] Elevated plasma CHGA levels are associated with clinical severity and serve as independent prognostic indicators in patients with complicated myocardial infarction,[4] acute coronary syndromes,[5] and chronic heart failure.[6]

CHGA also acts as a prohormone and gets cleaved to give rise to several bioactive peptides,[7] including vasostatin (human $CHGA_{1–76}$, a vasodilator and suppressor of inotropy/lusitropy),[8] pancreastatin (human $CHGA_{250–301}$, a dysglycemic hormone),[9]

Received April 21, 2016; first decision May 14, 2016; revision accepted May 17, 2016.

From the Department of Biotechnology, Bhupat and Jyoti Mehta School of Biosciences, Indian Institute of Technology Madras, Chennai, Tamil Nadu, India (M.Kiranmayi, V.R.C., P.K.R.A., L.S., B.S.S., R.K., M.D., S.Senapati, N.R.M.); Department of Molecular Cardiology, Lerner Research Institute, Cleveland Clinic, OH (E.E.M., S.V.N.P.); Department of Genetics, Dr. ALM PG Institute of Basic Medical Sciences, University of Madras, Taramani Campus, Chennai, Tamil Nadu, India (D.V., A.K.M.); Department of Experimental Medicine and Biotechnology, Postgraduate Institute of Medical Education and Research, Chandigarh, India (S.Sharma, M.Khullar); Department of Molecular Genetics, Madras Diabetes Research Foundation, Chennai, Tamil Nadu, India (D.B., V.R., V.M.); Institute of Cardiovascular Diseases, Madras Medical Mission, Chennai, Tamil Nadu, India (A.S.M.); Department of Medicine, University of California San Francisco (P.K.R.A.); and Department of Clinical Biochemistry, University of Cambridge, Cambridge, United Kingdom (B.S.S.).

The online-only Data Supplement is available with this article at http://hyper.ahajournals.org/lookup/suppl/doi:10.1161/HYPERTENSIONAHA.116.06568/-/DC1.

Correspondence to Nitish R. Mahapatra, Department of Biotechnology, Bhupat and Jyoti Mehta School of Biosciences, Indian Institute of Technology Madras, Chennai 600036, India. E-mail nmahapatra@iitm.ac.in

catestatin (CST; human $CHGA_{352–372}$, an antihypertensive and cardiosuppressive agent), parathyroid hormone release inhibitor parastatin (human $CHGA_{356–428}$),[10] and serpinin (human $CHGA_{411-436}$, a myocardial β-adrenergic–like agonist).[11] CST was discovered initially as a physiological brake of the adreno–sympathetic–chromaffin system because of its potent catecholamine release–inhibitory function,[12,13] which it manifests by acting specifically on the neuronal nicotinic acetylcholine receptor.[14,15] Plasma CST level is diminished in hypertensive individuals and even in the normotensive offspring of the established hypertensive patients, suggesting its pathogenic role in the development of hypertension.[16] Consistently, severe hypertension in *CHGA* knockout (and thereby, CST-lacking) mice is rescued by the exogenous administration of CST, revalidating its role as an antihypertensive molecule.[17] Many functionally active DNA variants have been discovered in the promoter, coding and 3′-untranslated regions of the human *CHGA* gene.[7,18] Resequencing of the CST-expressing region of *CHGA* in several human populations has revealed the occurrence of 5 single-nucleotide polymorphisms (SNPs; Table S1 in the online-only Data Supplement). A previous report from our laboratory has confirmed the presence of Gly364Ser (rs9658667) variation and, in addition, discovered a novel SNP, Gly367Val (rs200576557), in a Chennai (South India) population.[19] In this report, we analyzed the effect of the Gly364Ser variation on metabolic/cardiovascular disease states in a larger sample size (n=3200 individuals) in the Chennai population. As part of a replication study, we also genotyped the variant in a geographically/ethnically distinct North Indian population from Chandigarh (n=760 individuals). In both the populations, the 364Ser allele showed strong associations with elevated blood pressure (BP) levels and hypertension.

CST peptides have been found to dose dependently reduce the effect of β-adrenergic stimulation.[20] This reduction is mediated by a nitric oxide (NO)–releasing action of CST in endocardial endothelial cells, rather than a direct myocardial action of the peptide. Studies in the ex vivo models of Langendorff-perfused rat heart,[21] amphibian (*Rana esculenta*) heart,[22] and fish (*Anguilla anguilla*) heart[23] have also documented the antiadrenergic and cardiac inotropy/lusitropy modulatory effects of CST. On the basis of these observations, we questioned whether regulation of NO generation by CST peptides is because of their direct interactions/effects on β-adrenergic receptors (ADRB1/2). To understand the mechanistic basis of differential BP manifestations in the individuals because of CST peptides, we performed biochemical studies to assess NO generation, extracellular regulated kinase (ERK) activation, endothelial nitric oxide synthase (eNOS) phosphorylation, and the direct binding of CST peptides to ADRB1/2. In addition, we used a comprehensive set of computational tools including molecular modeling, docking, and molecular dynamics simulations to analyze the potential of CST-WT and CST-364Ser peptides to bind to ADRB1/2. CST-364Ser peptide exerted altered interactions with ADRB2 and led to diminished endothelial NO production (as compared with the CST-WT peptide), which may account for the increased risk for hypertension in 364Ser carriers.

Methods

The detailed methodologies are included in the online-only Data Supplement.

Human Subjects and Study Design

This case–control study recruited 3200 and 760 unrelated human volunteers in Chennai (South India) and Chandigarh (North India), respectively. The detailed demographic and clinical parameters are given in the Tables S2 and S3.

Each subject gave informed, written consent for the use of their blood samples for genetic and biochemical analyses in this study. This study was approved by the Institute Ethics Committee at Indian Institute of Technology Madras in accordance with Declaration of Helsinki (reference number: IITM IEC No 2007008).

The exon-7 region of *CHGA* was resequenced in 1763 subjects to detect the presence of SNPs in CST, pancreastatin, and parastatin domains. Another 2197 subjects were genotyped for the Gly364Ser SNP by Taqman allelic discrimination method. We also resequenced the *CHGA* promoter region in 581 study subjects using specific primers.[19]

Data Representation and Statistical Analysis

The experimental data results and the phenotypic characteristics in the human study are expressed as mean±SE. Allele frequencies were estimated by gene counting. A Pearson χ^2 test was used to compare the distribution of the genotypes. Statistical analysis was performed using the Statistical Package for Social Sciences version 21.0. Haploview 4.2 was used for linkage disequilibrium (LD) analysis.[24] A P value of <0.05 was chosen as statistically significant. The power of the study was calculated using Quanto version 1.2.4.[25] Meta-analysis was performed using the OpenMeta[Analyst] software (www.cebm.brown.edu/open_meta/).

Synthesis of CST Peptides

The CST wild-type (CST-WT, SSMKLSFRARAYGFRGPGPQL) and CST-364Ser variant (CST-364Ser, SSMKLSFRARAY**S**FRGPGPQL) peptides were synthesized by solid-phase method and purified as described previously.[19]

Measurement of NO Levels and eNOS Activity in Cultured Human Umbilical Vein Endothelial Cells

Experimental procedures involving umbilical cords were reviewed and approved by the Indian Institute of Technology Madras Institutional Ethics Committee in accordance with Declaration of Helsinki revised in 2000 (reference number: IITM IEC No 2009024). Human umbilical vein endothelial cells (HUVECs) were isolated from umbilical cords by digestion with collagenase as described previously.[26] NO levels in HUVECs were measured by 4, 5-Diaminofluorescein diacetate method as described previously.[27] Activation of eNOS in HUVECs by CST peptides was assessed by Western blotting and detection of phospho-eNOS-Ser^{1177}.

Isolation of ADRB1/2-Expressing Plasma Membranes, Radioligand Binding Assays, and Competition Binding Assays

Human Embryonic Kidney-293 (HEK-293) cells stably expressing ADRB1/2 were treated with isoproterenol and CST peptides. Activation of ERK as a measure of ADRB1/2-activation in ADRB1/2 HEK-293 cells was assessed by immunoblotting and detection of phospho-ERK as previously described.[28]

Purification of plasma membranes from control HEK-293 and ADRB1/2 HEK-293 cells was performed as previously described.[29,30] To test the level of ADRB1/2 expression, [^{125}I]-cyanopindolol saturation radioligand binding was performed on the isolated plasma membranes. Competition binding was performed by incubating 20 μg of plasma membranes with saturating concentrations of CST-WT and CST-364Ser peptides in the range of 10 pmol/L to 1 mmol/L.

Homology Modeling of ADRB1/2 Receptors and CST Peptides and Analysis of Peptide–Receptor Interactions

The crystal structure of ADRB2 with resolution 2.4 Å was obtained from protein data bank (PDB ID:2RH1).[31] The structure of ADRB1

was modeled by using the structure of ADRB2 as a template. The 3D structures of CST-WT and CST-364Ser were generated following a similar protocol as proposed earlier.[32] The residue Gly364 in the NMR (nuclear magnetic resonance) structure of CST (PDB ID:1LV4) was mutated to 364Ser using Modeller 9v13.[33] Short energy minimizations were performed on both the peptide structures to optimize the side-chain positions. The minimized structures were subsequently subjected to 300 ns explicit water molecular dynamics simulations to generate an ensemble of refined CST-WT and CST-364Ser conformations.

Protein–protein dockings of CST peptides on ADRB1/2 were performed using ZDOCK algorithm.[34] During molecular docking, CST peptides were allowed to search the extracellular region of the ADRB1/2 receptors to identify the best binding location. Out of the 100 binding modes of CST peptides to ADRB1/2, the best docked complex was identified based on the ZDOCK score.

All the structural figures were rendered using Visual Molecular Dynamics.[35] The CST–ADRB2 interactions were identified using PDBsum,[36] and cyanopindolol–ADRB2 interactions were identified using LigPlot+.[37]

Results

Discovery and Occurrence of the CST-Gly364Ser SNP in Indian Populations

Resequencing of the CST region of *CHGA* in 1763 subjects from an urban Chennai (South Indian) population consisting of type 2 diabetes mellitus (DM)/hypertension cases and controls led to discovery of 2 variants: Gly364Ser (rs9658667) and Gly367Val (rs200576557). Because the Gly364Ser variation was common (>5% minor allele frequency [MAF]), we genotyped additional 918 subjects for this SNP by Taqman allele discrimination method in the same population. We also genotyped the SNP in a population of 519 patients with coronary artery disease (CAD) from the same region (Chennai). The Gly364Ser SNP, which is caused by an A to G transition at the 9559 bp position leading to the substitution of codon GGC by codon AGC at the 364th amino acid position of the mature CHGA protein (Figure S1), was found to occur at 6.34% MAF, that is, in ≈13% of the study population (Table S4). We then performed a second replication study in a population from Chandigarh (North Indian) consisting of hypertensive cases and controls. Here, surprisingly, we found the SNP at a much lower MAF (3.48%), that is, only in ≈7% of the population, without the presence of a single homozygous variant in 760 individuals (Table S4).

Genotype frequencies were found to be in Hardy–Weinberg equilibrium (HWE) in the Chennai DM/hypertension (χ^2=1.286; *P*=0.256) population, Chennai CAD population (χ^2=0.250; *P*=0.617), Chandigarh hypertension population (χ^2=1.047; *P*=0.306), and Chandigarh controls population (χ^2=0.142; *P*=0.706). The Chennai controls population, however, showed a departure from Hardy–Weinberg equilibrium (χ^2=6.799; *P*=0.009). On closer observation of the genotypes in this population, we found that the presence of only 2 homozygous variants accounted for this departure.

364Ser Allele Is Associated With Hypertension in Independent Populations

The Chennai population was divided into different disease groups (DM, hypertension, and CAD), and logistic regression analysis was performed under both the genotype (GG versus AG and GG versus AA) and dominant (GG versus AG+AA) genetic models. Because of the small number of homozygous variant individuals (n=18), the recessive model was not used. Gly364Ser allele was found to be associated with hypertension under both the models, with unadjusted odds ratios (OR) of 1.440 (95% confidence interval [CI], 1.072–1.933; *P*=0.015) for GG versus AG and 1.385 (CI, 1.039–1.846; *P*=0.026) for GG versus AG+AA (Table 1). The associations retained significance even after adjusting individually for age, sex, and body mass index, as well as all 3 factors together (Table 1). An additional adjustment for antihypertensive medications along with age, sex, and body mass index also showed significant association for GG versus AG+AA at OR=1.694 (CI, 1.018–2.819; *P*=0.042). Interestingly, stronger associations of the 364Ser allele with hypertension were detected in a subgroup (having body mass index <24) of this population under both dominant genetic model (unadjusted OR, 1.856; CI, 1.234–2.792; *P*=0.003; age-adjusted OR, 1.983; CI, 1.312–2.997; *P*=0.001; and sex-adjusted OR, 1.856; CI, 1.227–2.809; *P*=0.003) and GG versus AG genotype model (unadjusted OR, 1.754; CI, 1.155–2.662; *P*=0.008; age-adjusted OR, 1.854; CI, 1.216–2.826; *P*=0.004; and sex-adjusted OR, 1.775; CI, 1.164–2.709; *P*=0.008). The 364Ser allele also showed higher frequency in subjects having any of the 3 disease states (DM/hypertension/CAD). Although the unadjusted ORs were not significant, adjustment with age yielded modestly significant ORs of 1.325 (CI, 1.024–1.714; *P*=0.032) and 1.299 (CI, 1.011–1.667; *P*=0.041) under the genotype and dominant models, respectively.

The replication population (Chandigarh) also showed strong association of the 364Ser allele with hypertension.

Table 1. Association of CST-364Ser Allele With Risk for Hypertension

Population	Genotype	OR (95% CI); *P* Value				
		Unadjusted	Age Adjusted	Sex Adjusted	BMI Adjusted	Age, Sex, and BMI Adjusted
Chennai	GG vs AG	1.440 (1.072–1.933); *P*=0.015	1.483 (1.103–1.994); *P*=0.009	1.431 (1.063–1.926); *P*=0.018	1.441 (1.072–1.938); *P*=0.015	1.469 (1.087–1.984); *P*=0.012
Chennai	GG vs AG+AA	1.385 (1.039–1.846); *P*=0.026	1.429 (1.070–1.907); *P*=0.015	1.380 (1.033–1.845); *P*=0.030	1.393 (1.043–1.858); *P*=0.025	1.424 (1.062–1.909); *P*=0.018
Chandigarh	GG vs AG	2.662 (1.420–4.990); *P*=0.002	2.951 (1.390–6.265); *P*=0.005	2.639 (1.389–5.013); *P*=0.003	n.c.	n.c.

Logistic regression analysis was performed in the Chennai and Chandigarh populations. Odds ratio for hypertension was analyzed. The analyses were done both by the genotype (GG vs AG and GG vs AA) and dominant (GG vs AG+AA) genetic models for the Chennai population. BMI indicates body mass index; CI, confidence interval; n.c., not calculable because of unavailability of BMI data in this study population; and OR, odds ratio.

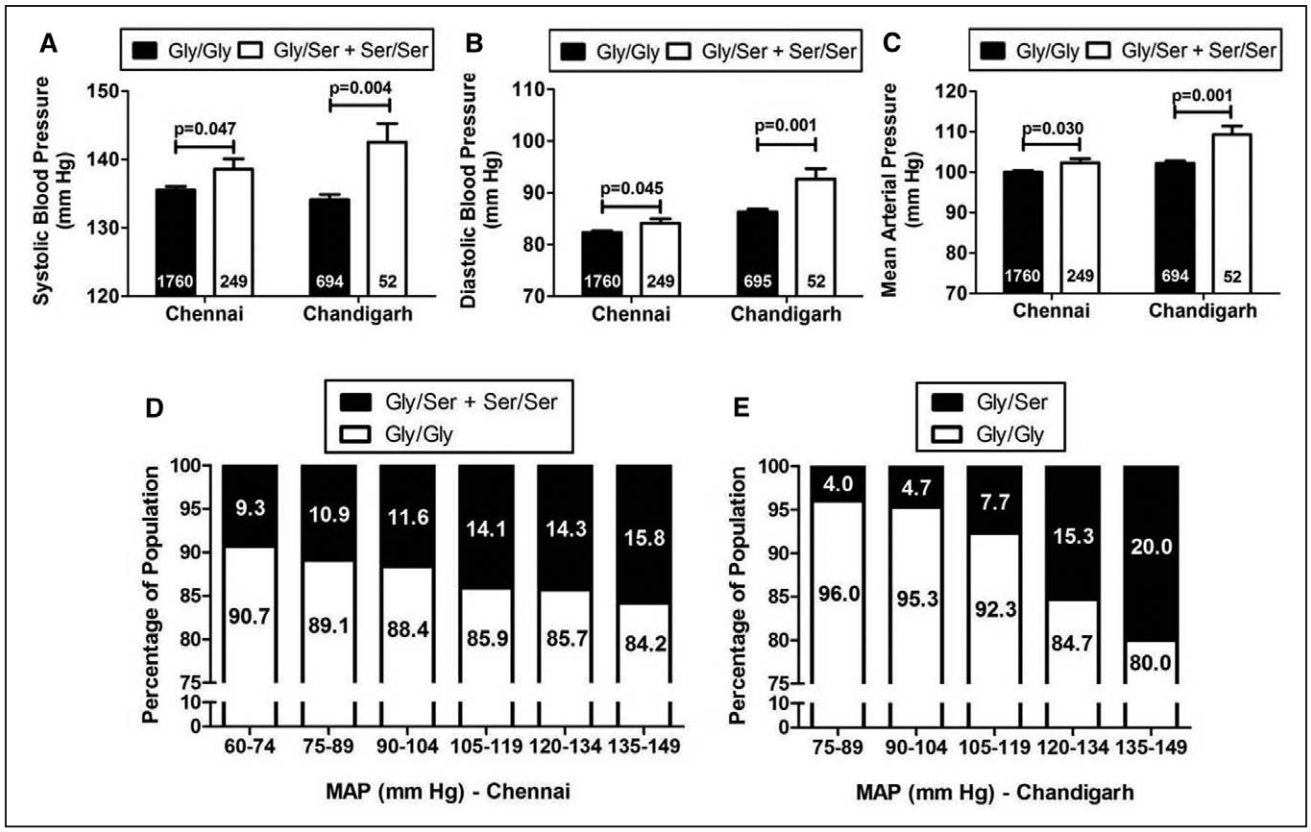

Figure 1. Allele-specific associations of the catestatin (CST) Gly364Ser variation with blood pressure. **A–C**, Data are shown as mean±SE. Systolic blood pressure (**A**), diastolic blood pressure (**B**), and mean arterial pressure (MAP; **C**) levels in the carriers of 364Ser allele were higher (analyzed by independent samples *t* test using SPSS version 21.0) than the wild-type individuals in the overall Chennai and Chandigarh populations. **D** and **E**, Data are shown as percentage. The percentage of individuals harboring the 364Ser allele showed an increase with increase in the range of the MAP levels in both the Chennai (**D**) and Chandigarh (**E**) populations.

Because there were no homozygous variant individuals identified in this population, the logistic regression analysis based on both genotype and dominant models yielded the same results. The unadjusted OR was highly significant at 2.662 (CI, 1.420–4.990; *P*=0.002; Table 1). The association persisted even after adjusting for age at OR=2.951 (CI, 1.390–6.265; *P*=0.005), sex at OR=2.639 (CI, 1.389–5.013; *P*=0.003), and age and sex together at OR=2.862 (CI, 1.359–6.028; *P*=0.006) (Table 1). Adjusting for smoking and dyslipidemia as well (data for which was not available for a large section of our study subjects) would have made this study stronger.

Association of 364Ser Variant With Elevated BP Levels in Independent Populations

In the primary Chennai population, there was a significant trend of increased BP levels in the carriers of the 364Ser allele as compared with the WT individuals. Initially, we compared the BP levels among the different genotype groups in 2069 individuals from the overall DM/hypertension population. The variant individuals had ≈2.5 mm Hg higher systolic BP (SBP; *P*=0.045), ≈1.5 mm Hg higher diastolic BP (DBP; *P*=0.074), and ≈2 mm Hg higher mean arterial pressure (MAP; *P*=0.043) levels than the WT individuals. Next, to adjust for the effect of the antihypertensive medications, 60 individuals without information for antihypertensive medication were removed, and the analysis was repeated after adjusting the BP values in the remaining 2009 individuals.[38] After drug adjustment, 364Ser carriers displayed ≈3 mm Hg higher SBP (*P*=0.047), ≈2 mm Hg higher DBP (*P*=0.045), and ≈2.5 mm Hg higher MAP (*P*=0.030) levels as compared with Gly364 carriers (Figure 1A–1C). Adjusting for age via ANCOVA further strengthened the association for SBP (*P*=0.031), DBP (*P*=0.044), and MAP (*P*=0.025; Table 2).

In the Chandigarh population as well, we found 364Ser to be associated with elevated BP levels. The variant allele–carrying individuals showed ≈8 mm Hg higher SBP (*P*=0.004), ≈6 mm Hg higher DBP (*P*=0.001), and ≈7 mm Hg higher MAP (*P*=0.001) levels than the WT individuals (Figure 1A–1C). For the hypertensive cases, the pretreatment BP levels were considered for association.

We further divided our Chennai and Chandigarh populations into different BP ranges and calculated the frequencies of the 364Ser allele in each range. With an increase in the severity of the disease, there was an increase in the percentage of people harboring the variant allele (for Chennai: linear-by-linear association χ^2=3.99 and *P*=0.046 and for Chandigarh: linear-by-linear association χ^2=12.89 and *P*=0.0003; Figure 1D and 1E).

The unadjusted power of the study for the hypertensive Chennai population was 65.6% and on adjusting for age, sex, and body mass index, the power of the study stood at 73.1%. For the Chandigarh population, the unadjusted power was 98.5%, whereas power adjusted for age and sex was 98.3%.

Table 2. Meta-Analysis of the 364Ser Allele Effects on Blood Pressure in Asian Populations

Population	Parameter	Gly/Gly			Gly/Ser+Ser/Ser			Effect Size	95% Confidence Interval		Unadjusted *P* Value	Adjusted *P* Value (ANCOVA)
		n	Mean	SEM	n	Mean	SEM		Lower Boundary	Upper Boundary		
Chennai/ South Indian	SBP	1760	135.50	0.54	249	138.57	1.52	3.07	–0.09	6.23	0.047	0.031
	DBP	1760	82.33	0.31	249	84.12	0.84	1.79	0.03	3.55	0.045	0.044
	MAP	1760	100.04	0.37	249	102.3	1.00	2.26	0.17	4.35	0.030	0.025
Chandigarh/ North Indian	SBP	694	134.12	0.76	52	142.54	2.70	8.42	2.92	13.92	0.004	0.009
	DBP	695	86.33	0.49	52	92.65	2.00	6.32	2.28	10.36	0.001	0.004
	MAP	694	102.24	0.55	52	109.29	2.07	7.05	2.85	11.25	0.001	0.003
Ibaraki, Saitama, Shizuoka/ Japanese	SBP	301	132.00	1.14	42	138.20	2.72	6.20	0.42	11.98	0.055	0.048
	DBP	301	80.30	0.60	42	82.00	1.37	1.70	–1.23	4.63	0.314	n.s.
	MAP	301	100.7	0.86	42	104.50	1.97	3.80	–0.41	8.01	0.117	n.s.
	PP	301	51.70	0.72	42	56.10	1.92	4.40	0.382	8.418	0.030	0.025
Overall population	SBP	2755	…	…	343	…	…	5.21	1.92	8.50	<0.01	…
	DBP	2756	…	…	343	…	…	2.76	0.40	5.11	0.02	…
	MAP	2755	…	...	343	…	…	3.93	1.12	6.73	<0.01	…

Meta-analysis was performed using the data for the effect size of the Gly364Ser SNP in the 3 Asian populations of Chennai, Chandigarh, and Japan. The data for the Japanese population were derived from the study by Choi et al.[59] Age-adjusted ANCOVA was performed in the Chennai and Chandigarh populations. For the Japanese population, the ANCOVA was performed considering gender, age, BMI, antihypertensive medication, diabetes, dyslipidemia, and smoking as covariates. The three independent populations displayed directionally concordant effect on blood pressure. Meta-analysis results show an overall significant effect of elevated blood pressure in 364Ser allele carriers. BMI indicates body mass index; DBP, diastolic blood pressure; MAP, mean arterial pressure; PP, pulse pressure calculated from SBP and DBP; n.s., not significant; and SBP, systolic blood pressure.

364Ser Allele Is in LD With *CHGA* Promoter SNPs and Neighboring Exon-7 Coding Variants

Previous studies have discovered the occurrence of common SNPs in the *CHGA* promoter as well as coding regions.[18,19,39] Many of these SNPs have been found to be functionally active, either in altering the transcriptional activity of the promoter[18] or the potencies of the peptides they are found in.[18,32,39,40] We had the complete genotyped data for 581 individuals for the Gly364Ser SNP, 8 *CHGA* promoter SNPs: -1106G→A (rs9658628), -1018A→T (rs9658629), -1014T→C (rs9658630), -988T→G (rs9658631), -462G→A (rs9658634), -415T→C (rs9658635), -89C→A (rs7159323), and -57C→T (rs9658638); and 3 other neighboring SNPs in the *CHGA* exon-7: Gly297Ser (rs9658664), Arg381Trp (rs729940), and Glu403Glu (rs729939). To test whether the Gly364Ser variant is likely to be segregated with any of these other common SNPs, and whether association with the variant is also being contributed by them, we performed an LD analysis using the genotyped data for the 581 subjects. The Gly364Ser variant was found to be in LD with 7 out of the 11 polymorphisms: 4 in promoter (-1106G→A, -1018A→T, -415T→C, and -57C→T) and 3 in *CHGA* exon-7 (Gly297Ser, Arg381Trp, and Glu403Glu; Figure S2).

CST Peptides Differ in NO Production Ability in HUVECs

To investigate the increase in BP levels in the presence of the 364Ser allele, we tested whether the WT and variant peptides differ in their efficacies in inducing NO production in vascular endothelial cells. Initially, we treated HUVECs with 2 doses of CST-WT (0.1 and 1 nmol/L), both of which significantly increased (P<0.001) the NO levels as compared with the basal condition (Figure 2A). The NO indices followed the order: 1 nmol/L CST-WT (2.50) > 0.1 nmol/L CST-WT (2.35) > basal (1.90) (Figure 2B). Because at both the doses the peptide showed significant effect, we then chose to continue with a dose of 1 nmol/L to compare the activities of the variant and the WT peptide. Treatment of HUVECs with CST-WT or CST-364Ser showed that NO indices were increased with both the peptides compared with basal (P<0.001), but however, the increase with CST-WT was significantly higher than CST-364Ser variant (P<0.001; Figure 2C). The NO indices in HUVECs were in the following order: CST-WT (22.85) > CST-364Ser (19.26) > basal (16.85) (Figure 2D). Interestingly, when both the peptides were added in an equimolar ratio as a representative of the heterozygous condition, the NO index (19.89) was in between that of the WT and variant peptide (Figure 2C and 2D).

In view of the direct links between stimulation of cardiovascular β-adrenergic receptors and NO generation,[41] we sought to test whether the NO effects of the CST peptides are routed through their interactions with the β-adrenergic receptors ADRB1 and ADRB2. Accordingly, we treated HUVECs with ADRB1/2 antagonists (viz CGP 20712 for ADRB1 and ICI 118551 for ADRB2), followed by treatment with the CST peptides. The ADRB2 antagonist was found to significantly blunt the NO-increasing effect of the CST-WT peptide (NO index for CST-WT: 9.09 versus NO index for CST-WT+ICI 118551: 8.01), whereas it did not do the same in the case of CST-364Ser peptide (NO index for CST-364Ser: 8.80 versus NO index for CST-364Ser+ICI 118551: 8.36; Figure 2E and

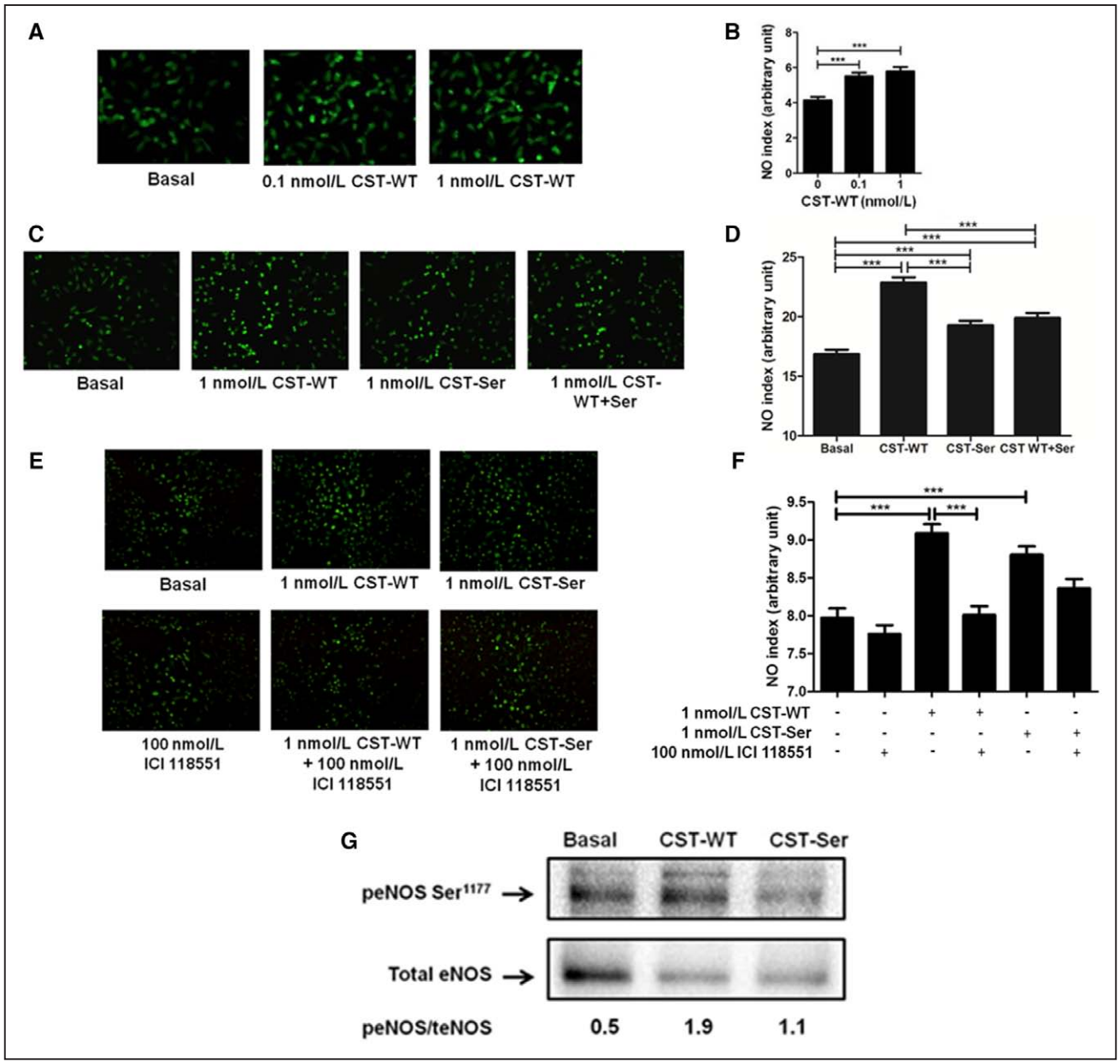

Figure 2. Effect of catestatin (CST) peptides on NO production in human umbilical vein endothelial cells (HUVECs). The fluorescence intensities (NO indices) were calculated by Image J analysis and plotted as mean±SE. The experimental groups were compared by 1-way ANOVA followed by Tukey multiple comparison post-test. **A** and **B**, Representative images for the treatment of HUVECs with different doses of CST wild-type peptide (CST-WT; 0.1 nmol/L and 1 nmol/L). ***P<0.001; 1-way ANOVA F=15.71 and P<0.0001; n=50 cells per condition. **C** and **D**, Representative images for the treatment of HUVECs with CST peptides. ***P<0.001; 1-way ANOVA F=37.15 and P<0.0001; n=450 cells per condition. The order for efficacy of peptides in NO production: CST-WT>CST-WT+Ser>CST-364Ser>basal. **E** and **F**, Representative images for the treatment of HUVECs with CST peptides and ADRB2 antagonist ICI 118551. ***P<0.001; 1-way ANOVA F=19.65 and P<0.0001; n=450 cells per condition. **G**, Representative Western blot of 3 independent experiments showing phosphorylated Ser^{1177}-eNOS (peNOS) and total eNOS (teNOS) levels on treatment of HUVECs with CST peptides. The peNOS/teNOS values have been indicated below each lane.

2F). ADRB1 antagonist failed to show any inhibition of the NO levels produced by both peptides (Figure S3).

Next, to assess the effect of CST peptides on eNOS activity, we checked the phosphorylation levels of eNOS at Ser^{1177} residue, after treatment with the CST peptides. CST-WT increased the phosphorylation at Ser^{1177} of eNOS as compared with CST-364Ser (Figure 2G). Because phosphorylation at Ser^{1177} leads to activation of eNOS, these results suggest an overall higher eNOS activity in cells treated with CST-WT.

Differential Interactions of CST Peptides With ADRB1/2: Experimental Evidence

We then tested the interactions of the CST peptides with ADRB1/2 to see whether their altered interactions with either of the receptors can explain their differential NO effects. Competition binding assays were performed with [^{125}I]-cyanopindolol using HEK-293 cells stably expressing human ADRB1/2. The levels of ADRB1/2 expression were assessed by performing radioligand binding using saturating concentrations of [^{125}I]-cyanopindolol

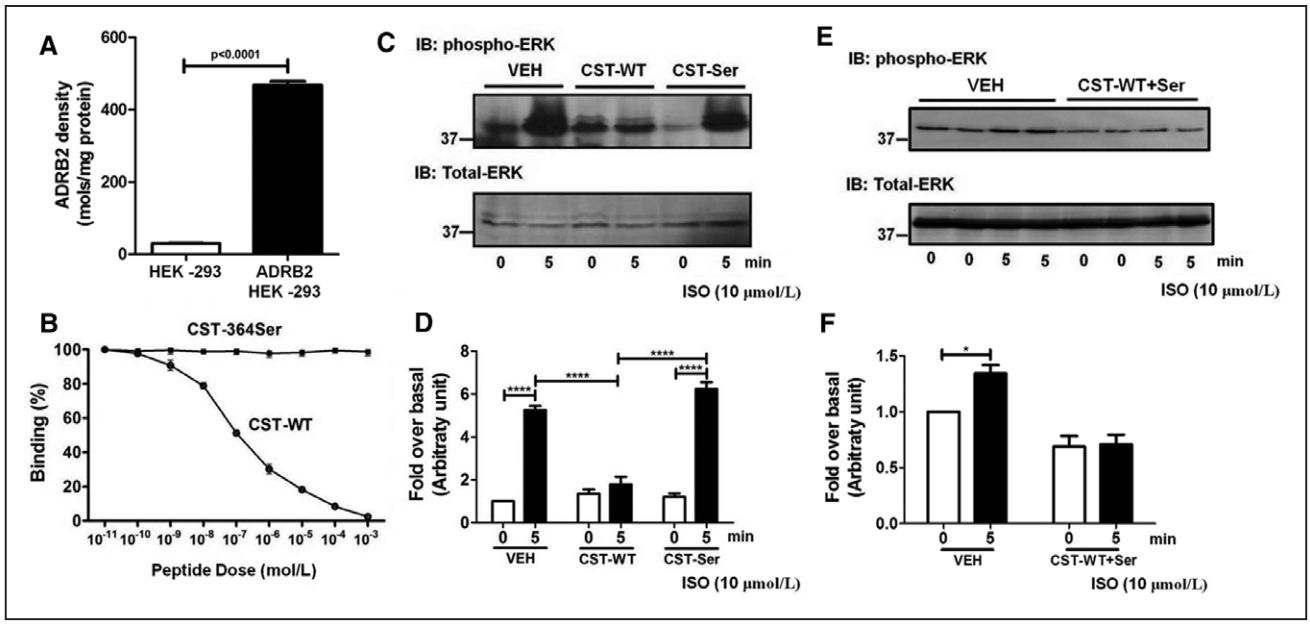

Figure 3. Binding of catestatin (CST) peptides to ADRB2 receptor and downstream effects. **A**, ADRB2 HEK-293 cells showed ≈16-fold higher expression of ADRB2 (P<0.0001 by 2-tailed unpaired t test) as compared with control HEK-293 cells. Data are shown as ADRB2 levels normalized with total protein. **B**, Data are shown as percentage binding of the radioligand cyanopindolol. With increasing doses of CST wild-type peptide (CST-WT; 10 pmol/L to 1 mmol/L), the ligand got completely displaced (P<0.0001; F=2300; R^2=0.998), whereas with increasing doses of CST-364Ser, there was no effect. The experimental groups were compared by 1-way ANOVA followed by Tukey multiple comparison post-test. **C** and **D**, Representative western blot (**C**) and quantitative representation of the densitometric analysis from 4 to 6 independent experiments (**D**) showing phosphorylated ERK (pERK) and total ERK levels on treatment with CST peptides and isoproterenol (ISO). ISO (10 μmol/L) showed an increase in pERK levels at 5 minutes in the vehicle (VEH) condition, reflecting the activation of ADRB2. However, this increase was inhibited on pretreatment with CST-WT (10 μmol/L). ****P<0.0001. On the contrary, pretreatment with CST-364Ser (10 μmol/L) showed levels of activation similar to the vehicle. The experimental groups were compared by 2-tailed t test. **E** and **F,** Representative Western blot (**E**) and quantitative representation of the densitometric analysis from 4 independent experiments (**F**) showing pERK and total ERK levels on treatment with equimolar ratios of CST-WT and CST-364Ser peptides and ISO. ISO (10 μmol/L) showed an increase in pERK levels at 5 min in the vehicle (VEH) condition. However, this increase was inhibited upon pretreatment with CST-WT+Ser (10 μmol/L). *P<0.05. The experimental groups were compared by 2-tailed t test. IB indicates immunoblotting.

on plasma membranes isolated from ADRB1/2-expressing HEK-293 cells. ADRB1 HEK-293 cells showed ≈109-fold (P<0.0001) higher levels of ADRB1 expression (Figure S4A) because HEK-293 cells have very sparse endogenous expression of ADRB1. ADRB2 HEK-293 cells showed ≈16-fold (P<0.0001) higher level of ADRB2 expression compared with control HEK-293 cells (Figure 3A) because HEK-293 cells do have some level of endogenous ADRB2s. Plasma membranes from ADRB1/2 HEK-293 cells were then subjected to an indirect competition ligand-binding assay wherein we tested for the ability of increasing doses (10 pmol/L to 1 mmol/L) of CST-WT or CST-364Ser peptides to displace saturating concentrations of labeled cyanopindolol. In ADRB2 HEK-293 cells, CST-WT peptide competitively displaced the [^{125}I]-cyanopindolol with increasing concentrations (P<0.0001; F=2300; R^2=0.998) in contrast to CST-364Ser peptide which did not displace or compete with cyanopindolol (Figure 3B). However, in ADRB1 HEK-293 cells, both the peptides failed to displace [^{125}I]-cyanopindolol with increasing concentrations (Figure S4B).

To further check whether binding of these peptides has consequences in β-adrenergic signaling, receptor activation was assessed by determining the phosphorylation status of ERK. ADRB1/2 HEK-293 cells were pretreated with either CST-WT or CST-364Ser peptide followed by ADRB agonist isoproterenol stimulation. Although in ADRB2 HEK-293 cells, pretreatment with CST-WT inhibited ADRB2-mediated ERK activation (P<0.0001), CST-364Ser had no appreciable effects in altering ERK (Figure 3C and 3D). Interestingly, treatment with equimolar ratios of CST-WT and CST-364Ser elicited a similar response to that of CST-WT alone (Figure 3E and 3F). In ADRB1 HEK-293 cells, on the contrary, both the peptides failed to show any detectable effects in altering ERK levels (Figure S4C and S4D). These studies suggest that CST-WT may be acting as an inhibitor/antagonist to ADRB2 function in contrast to CST-364Ser which does not alter the ADRB2 function. Moreover, this differential effect seems to be limited to the ADRB2 receptor only and not the ADRB1 isoform.

Structures of the CST Peptides and Their Differential Interactions With ADRB1/2: Computational Analysis

To explore whether the differential effects of the peptides in vitro can be attributed to any structural differences between them, we generated in silico models of CST peptides and CST-ADRB1/2 complexes and performed structural analysis on them using protein–protein modeling and molecular dynamics simulations (Figure 4). The CST-WT structure was found to comprise a metastable antiparallel β-sheet and a random coil (Figure 4A). Its N-terminal β-strand was stabilized by interactions between Lys355, Leu356, and Ser357, whereas the C-terminal β-strand was stabilized by Gly369, Pro370, and Gln371. Interestingly, the mutation of Gly364 to 364Ser drastically changed the secondary

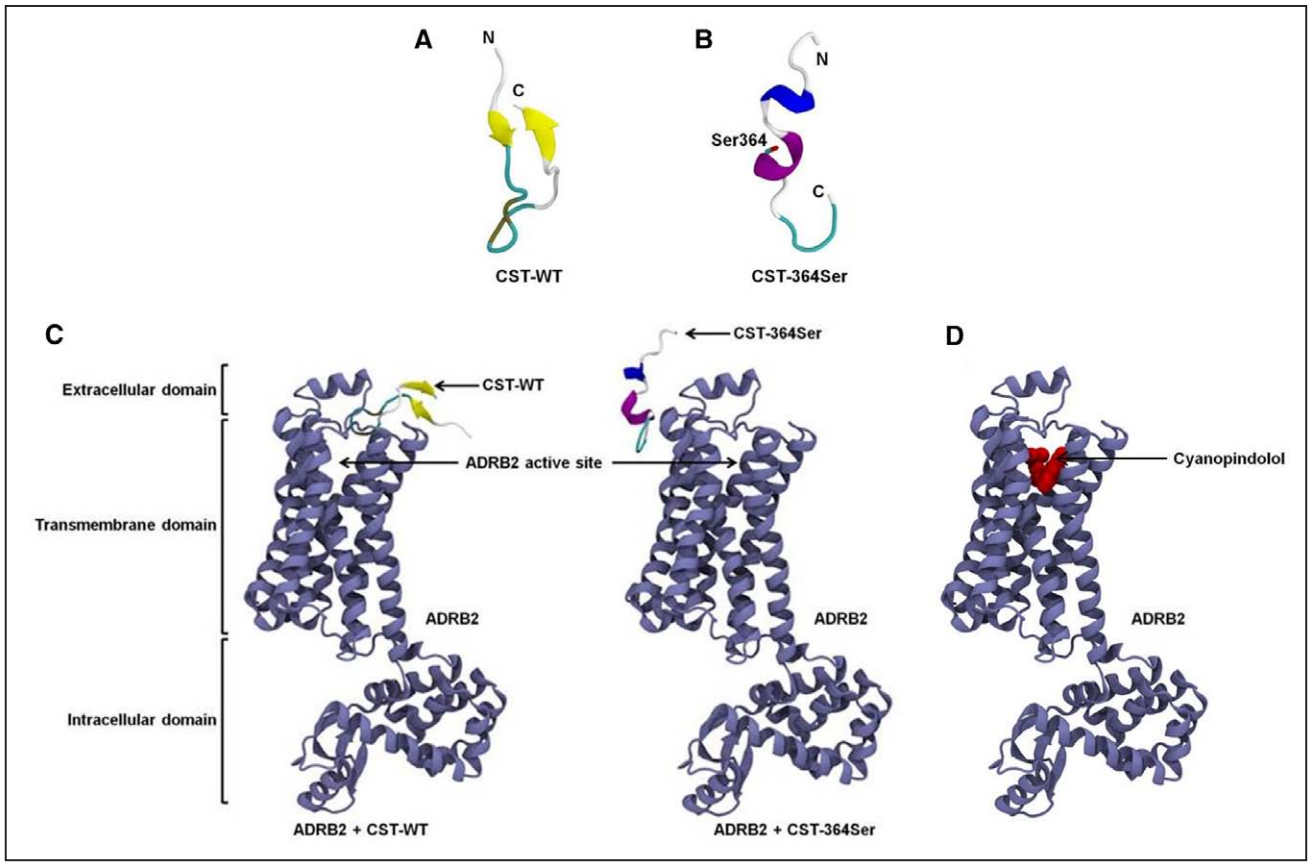

Figure 4. Structures of catestatin (CST) peptides and complexes of CST peptides/cyanopindolol with ADRB2 receptor. The time-averaged structures of CST-WT (**A**) and CST-364Ser (**B**) are shown in cartoon representation. The 364Ser mutation in the CST-364Ser peptide is shown in a stick representation. **C**, Snapshots of CST-WT (**left**) and CST-364Ser (**right**) docked to ADRB2. ADRB2: violet, β-sheet in CST-WT: yellow, α-helix in CST-364Ser: purple, and 3_{10} helix in CST-364Ser: blue. **D**, Snapshot of the docked complex of cyanopindolol (red, van der Waals representation) and ADRB2 (violet, cartoon representation).

structural content of CST. CST-364Ser displayed a metastable 3_{10} helix and a stable α-helix in the central region (Figure 4B). The 3_{10} helix was stabilized by residues Leu356, Ser357, and Phe358, and the stable α-helix comprised Arg361, Ala362, Tyr363, and Ser364. All residues of the time-averaged structures of both peptides from simulations are in the allowed regions of the Ramachandran plot (Figure S5), thus validating the proposed models of the peptides.

The binding of CST peptides to ADRB1/2 was explored via protein–protein docking in which both CST-WT and CST-364Ser were allowed to sample the extracellular region of the modeled ADRB1/2 (Figure S6) independently. In case of ADRB1, both the CST peptides did not show any significant binding to the ADRB1 active site (Figure S7). On the contrary, in case of ADRB2, they were found to bind to different locations of the receptor (Figure 4C). Although the thumb-like structure of CST-WT could fit into the ligand entry site of ADRB2 because of its shape complementarity, CST-364Ser failed to dock into the ligand entry site because of its linear stretched structure and difference in secondary structural content compared with CST-WT. It instead bound to the outer surface of the receptor, away from the CST-WT binding site. A brief 50 ns molecular dynamics simulation was performed on each of these CST-ADRB2 complexes in lipid bilayer for further refinement, but no significant change in binding mode was observed. The ZDOCK score (calculated based on surface complementarity, electrostatistics, and statistics potential) was 1197 for CST-WT and ADRB2 and 1067 for CST-364Ser and ADRB2, implying better binding of CST-WT to ADRB2.

To reconfirm the binding of CST-WT to ADRB2, the high-affinity ligand cyanopindolol was docked to the peptide–receptor complexes. In >100 attempts for protein-ligand docking through AutoDock,[42] cyanopindolol could never bind to the CST-WT–ADRB2 complex, whereas it bound effectively to the CST-364Ser–ADRB2 complex in all the attempts. This further proves the complete occlusion of the receptor's ligand-binding pocket by CST-WT and out-of-pocket binding of CST-364Ser to ADRB2 (Figure 4C).

To check the competitive binding of CST-WT and cyanopindolol to ADRB2, we produced the cyanopindolol–ADRB2 complex by protein-ligand docking (Figure 4D). Similar to the available crystal structure of cyanopindolol–ADRB1 complex (PDB ID: 4BVN),[43] cyanopindolol was found to bind to the hollow region of ADRB2 formed by the 7 transmembrane helices. A closer look at the interactions involved in the CST-WT–ADRB2 and cyanopindolol–ADRB2 complex formation revealed that even though cyanopindolol binds deep into the pocket, there were 2 common ADRB2 residues (viz Phe165 and Thr167) which interacted with both CST-WT (Figure 5A) and cyanopindolol (Figure 5C). Of note,

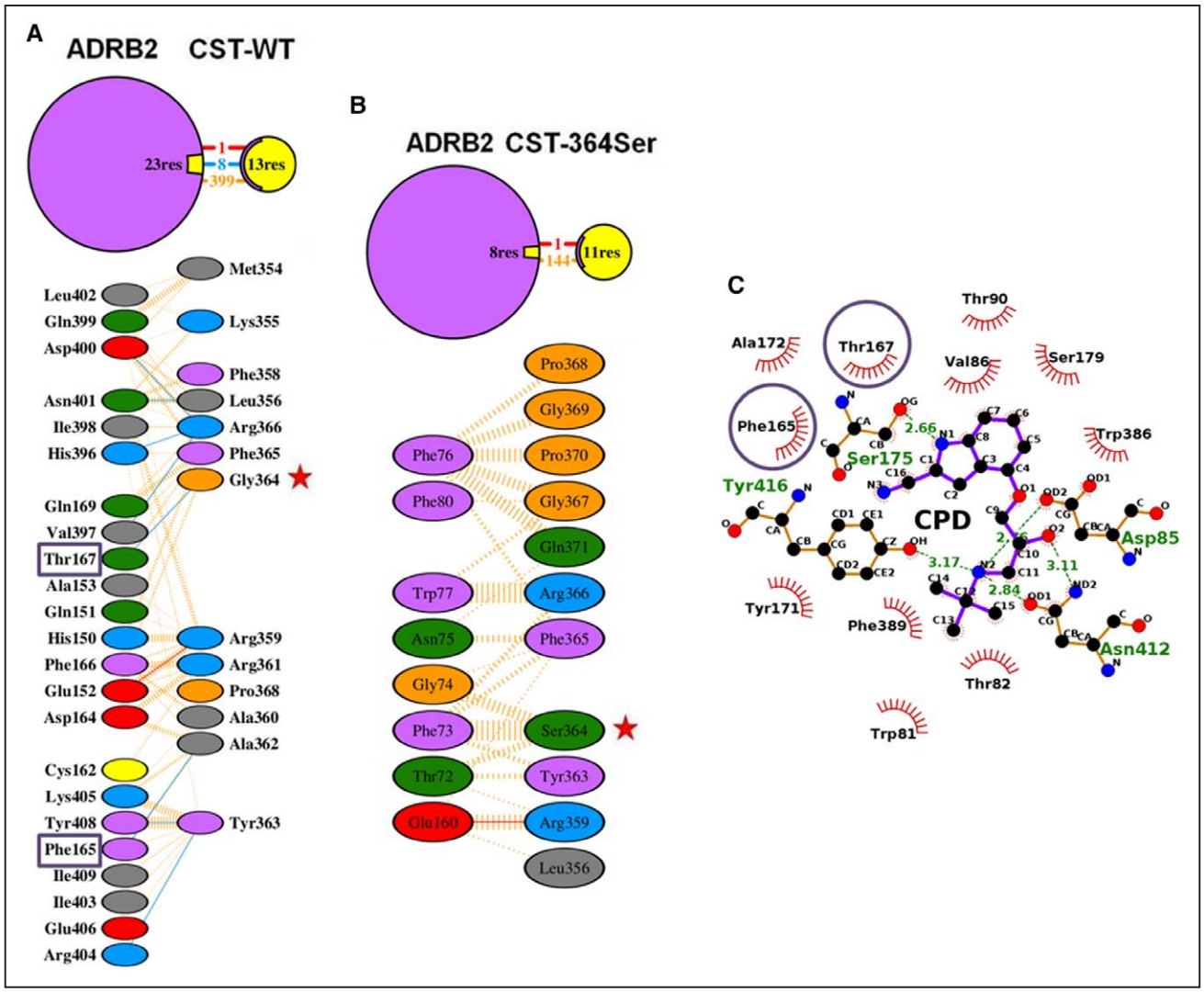

Figure 5. Molecular interactions in the complexes of catestatin (CST) peptides or cyanopindolol with ADRB2. **A** and **B**, Binding interactions in CST-WT–ADRB2 (**A**) and CST-364Ser–ADRB2 (**B**) complexes. Hydrogen bonds: blue lines, hydrophobic contacts: orange lines, and salt bridges: red lines. Each residue is color coded based on its nature with aliphatic residues in gray; aromatic residues in pink; negatively charged residues in red; positively charged residues in cyan; neutrally charged residues in green; Pro and Gly in orange; and Cys in yellow. Gly364Ser polymorphism: red stars. **C**, Binding interactions of cyanopindolol with ADRB2. Hydrophobic interactions: red spiked semicircles and hydrogen-bonding interactions: green dotted lines with distance values indicated. Common interacting residues of ADRB2 with CST-WT and cyanopindolol are highlighted using purple boxes in (**A**) and purple circles in (**C**), respectively.

ADRB2:Thr167 interacts with CST-WT:Gly364 strongly through hydrogen bonds during the CST-WT–ADRB2 complex formation, thus making CST-WT:Gly364 a crucial residue for complex formation. Therefore, it is not surprising that a mutation at this particular residue of CST makes its binding to ADRB2 active site weaker or there is no binding. The interactions in the CST-364Ser–ADRB2 complex formation involve 0 hydrogen bonds (in contrast to 8 in CST-WT–ADRB2 complex) and 1 salt bridge. The remaining interactions are hydrophobic in nature, including the ones involving 364Ser, making this binding a weak one (Figure 5B). An analysis of the Gly364Ser mutation using the polyphen-2 tool (which estimates the possible impact of an amino acid substitution on the structure and function of a human protein with the help of sequence, phylogenetic, and structural information characterizing the substitution) predicted this particular SNP to be possibly damaging with a score of 0.528 (sensitivity: 0.8; specificity: 0.9).[44]

Discussion

CST: A *CHGA*-Derived Antihypertensive Peptide

Recent studies have provided ample evidence to testify CST as a multifunctional peptide with diverse roles in the regulation of cardiovascular/metabolic functions.[45,46] Given that its precursor *CHGA* is a candidate gene for essential hypertension,[47] CST's role as an antihypertensive agent has been an interesting topic of research. The primary evidence for this was found when the administration of exogenous CST resulted in the rescue of the hypertensive and hyperadrenergic phenotypes exhibited by *CHGA* knockout mice.[17,48] The role of CST as a potent vasodilator in vivo has also been well documented both in rats[49] and in humans.[50] CST also seems to be capable of modulating the components of the brain-stem circuitry (rostral and caudal ventrolateral medulla) that regulate BP.[51,52]

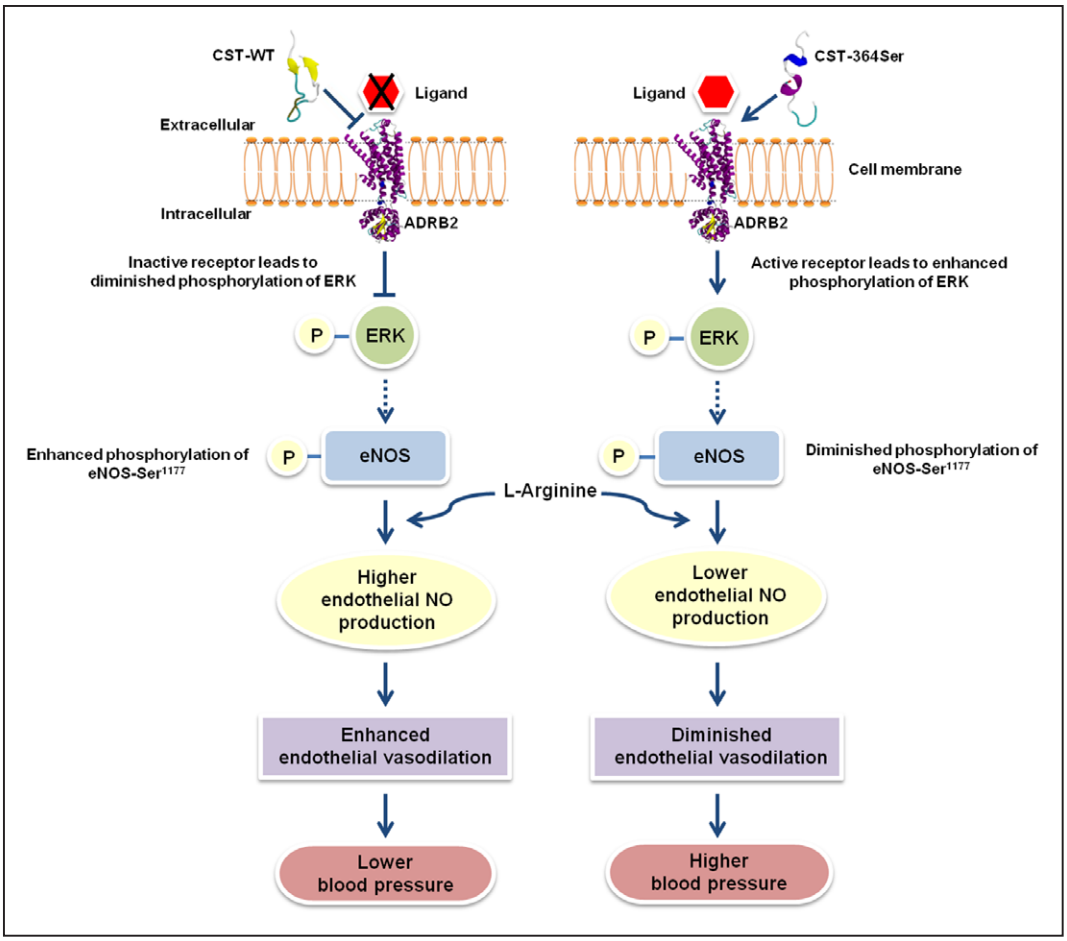

Figure 6. A schematic representation of the plausible mechanistic basis for the effects of catestatin (CST) peptides on blood pressure via modulation of NO pathway. The CST-364Ser peptide does not interact at the ligand-binding site of ADRB2 unlike CST-WT because of differences in their secondary structures. Their differential interactions with ADRB2 result in diminished antagonization of ADRB2 and enhanced activation/phosphorylation of extracellular regulated kinase (ERK) by CST-364Ser. The altered ERK activation between the CST peptides may result in diminished phosphorylation of eNOS-Ser^{1177} and consequently lower endothelial nitric oxide synthase (eNOS) activity in the case of CST-364Ser. These cellular/molecular processes lower the NO levels in vascular endothelial cells in the carriers of CST-364Ser allele leading to endothelial dysfunction and thereby increasing their risk for hypertension.

The Occurrence of the Gly364Ser SNP in Diverse Ethnic World Populations

The discovery of a functionally active variant of CST (Gly364Ser) in a Southern Californian population held promise of providing small, yet important, clues in elucidating the mechanism for the development of hypertension.[18] However, because of the vast difference in the genetic makeup of the different ethnic populations across the world, it would be irrational to generalize the magnitude and direction of allelic effect sizes across populations.[53,54] A study in the Population Architecture using Genomics and Epidemiology (PAGE) consortium of multi-ancestry populations has ably demonstrated that differential LD between common polymorphisms (tagSNPs) and functional variants within diverse populations significantly contribute to diluting the effect sizes among these populations.[55] The immense variation in the distribution of genotypes for the Gly364Ser polymorphism in different world populations foreshadows a similar distortion in the effect sizes in these populations (Table S5). Overall, the SNP seems to be occurring in 3 strata of ethnic groups. The first stratum, with a high allelic frequency (6% to 8%), includes the Asian and Hispanic groups. The European ethnicity forms the second stratum, which has a moderate frequency (2% to 5%). The third stratum, with the lowest frequency (0% to 1%), consists of the African populations. In our previous study,[19] we reported the discovery of the Gly364Ser polymorphism in an urban Chennai population (n=1010 individuals) at an MAF of ≈8.0%. In this study, we have expanded the sample size to 3200 individuals consisting of DM/hypertension/CAD/controls from the same population. 364Ser allele displayed an MAF of 6.34% in the Chennai DM/hypertension/CAD population, which seems to be consistent with the frequencies observed in other Asian populations. Interestingly, the ethnically distinct Chandigarh population displayed a much lesser MAF of 3.48%, which is closer to that observed in the European stratum than the Asian one. The distribution of the genotype frequencies differed significantly between Chennai DM/hypertension/CAD population and Chandigarh population (χ^2=18.01 and P=0.0001). Thus, CST region of *CHGA* seems to be displaying significant genetic variations among different world ethnic populations. In the evolutionary context,

the 364Ser variant has not been detected in other mammals (Figure S8). Some mammals (eg, Giant panda), however, have Asp at the 364th position.

Association of the CST-364Ser Allele With Hypertension

The logistic regression analysis revealed a significant association of the 364Ser allele with hypertension in both the primary (Chennai) and the replication (Chandigarh) populations (Table 1). This was supported by the observation of elevated BP levels in the 364Ser carriers in both the study populations. Despite the difference in the frequency of the Gly364Ser polymorphism in these 2 ethnically distinct populations, its effect on BP levels seems to replicate well. The higher occurrence of the variant allele in the population with an increase in BP ranges further provides the evidence of association of the 364Ser allele with hypertension (Figure 1D and 1E). Overall, the 364Ser allele seems to act as a risk allele for hypertension development in Indian populations.

Why has Gly364Ser not been detected in the genome-wide association studies performed on cardiovascular diseases till date? First, most of these genome-wide association studies were performed in either European or American populations wherein the MAFs for this SNP are much lower than those in Indian populations (Table S5). Because of the low MAFs, large sample sizes would be required to identify any significant association with this SNP in these populations. Second, almost all the genechip arrays (for example, Illumina Human550K Bead chip and Illumina Human610K Bead chip) used in these reported studies as well as other studies performed among Asians[56,57] did not harbor the Gly364Ser SNP. Therefore, the fact that these genome-wide association studies did not identify Gly364Ser as a risk variant for hypertension is not surprising.

We found the 364Ser allele to be in LD with the *CHGA* promoter SNPs at -1106, -1018, -415, and -57 bp positions (Figure S2). The 8 SNPs in the *CHGA* promoter form haplotypes which differ from each other in terms of their transcriptional activity.[18] The minor alleles at -1018, -415, and -57 bp positions of the *CHGA* promoter give rise to one of the 5 common *CHGA* promoter haplotypes (GTTTGCCT) which shows higher promoter activity as compared with the WT consensus haplotype (GATTGTCC).[18] This would mean that the 364Ser carriers may have a more active promoter leading to greater levels of the parent CHGA molecule being produced. Elevated levels of CHGA are associated with elevated BP levels.[58] Therefore, the hypertensive effect of the 364Ser allele might be getting manifested through increased *CHGA* promoter activity as well. 364Ser allele is also in modest LD with Gly297Ser, a functionally active SNP in pancreastatin that seems to alter the risk for type 2 diabetes mellitus in an Indian population.[32] Thus, the association of the 364Ser allele with elevated plasma glucose levels (Figure S9) may be an effect of it being a bystander.

Of note, in a Southern Californian population, the 364Ser allele displayed association with diminished DBP levels, especially in men; however, the effect was not consistently observed for SBP or in women.[39] Conversely, the 364Ser allele was associated with elevated SBP and MAP levels in a Japanese population (Table 2).[59] Thus, 364Ser allele seems to exert directionally concordant effects on BP in several Asian populations (South Indian, North Indian, and Japanese) although not in Caucasians. This is similar to a previous study reporting that the 12Ala allele in the peroxisome proliferator–activated receptor-γ2 did not offer the same protective role in Indians as it did in Caucasians.[60] Such contradictory associations of an allele provide evidence for heterogeneity in different populations and underscore the need for carrying out association studies in diverse ethnic populations to draw more accurate conclusions in each population.

Mechanistic Basis for Elevated BP Level in the Carriers of 364Ser: Influence of the Endothelial NO Pathway

It is well established that the endothelium plays an important role in regulating arterial BP. The manifestation of hypertension through impaired endothelium-dependent vasodilation as well as reduced NO production has been well documented in both animal[61,62] and human[63,64] studies. It is, therefore, not surprising that the hypertensive and hyperadrenergic phenotype in the *CHGA*-KO mice was accompanied by lowered NO levels.[65] The attenuation of such a phenotype on the exogenous administration of CST would therefore have to route through restoration of NO levels. In a study performed in BAE-1 (bovine aortic endothelium) cells,[20] CST-WT was shown to induce a wortmannin-sensitive, Ca^{2+}-independent increase in NO production and eNOS Ser^{1179} phosphorylation, whereas CST-364Ser was found to be ineffective. CST-WT has also been shown to dose dependently induce a NO-cGMP dependent cardiosuppression in the in vitro frog heart.[66] In light of this, we asked whether CST-WT and CST-364Ser differ in their ability to generate NO in HUVECs. Indeed, CST-364Ser displayed lower efficacy to produce NO in HUVECs (Figure 2D), thus corroborating the elevated BP levels in the 364Ser allele–carrying individuals. Consistently, carriers of 364Ser allele showed diminished (by ≈1090 mm/s) brachial artery pulse-wave velocity (indicating increased endothelial dysfunction) in a Japanese population.[59] eNOS is known to be activated via phosphorylation at its Ser^{1177} residue[67,68] HUVECs treated with CST-WT showed increased levels of phosphorylation at Ser^{1177} sites of eNOS as compared with HUVECs treated with CST-364Ser (Figure 2G). In case of CST-WT, there was a ≈3.8-fold increase in Ser^{1177} phosphorylation levels over basal; CST-364Ser, on the other hand, showed only a ≈2.2-fold increase in Ser^{1177} phosphorylation levels over basal. This is indicative of increased eNOS activity in case of CST-WT as compared with CST-364Ser which goes in corroboration with our observations of increased NO levels on treatment with CST-WT as compared with CST-364Ser in HUVECs.

Direct links between stimulation of cardiovascular β-adrenergic receptors and NO generation in endothelial cells are well established.[41] In isolated human umbilical vein, the vasorelaxation response to either the nonselective β-adrenergic agonist isoproterenol or to the cAMP analogue dibutyryl cAMP is attenuated by the NOS inhibitor NG-monomethyl-L-arginine. Thus, the β-adrenergic receptor–mediated vasorelaxation response in this system seems to be largely NO dependent and mediated through the elevation of cAMP

levels.[69] Likewise, in HUVECs as well, it has been shown that either β-adrenergic receptor–stimulated or β-adrenergic receptor–independent elevation of intracellular cAMP levels results in increased NOS activity.[69] In HUVECS, the inhibition of eNOS activity in the presence of the ADRB2 antagonist ICI 118551 and not ADRB1 antagonist CGP 20712 shows that this effect is mediated exclusively through ADRB2.[70] Consistently, we found that the elevation in NO levels mediated by CST-WT peptide was abrogated in the presence of ICI 118551 but not CGP 20712 (Figure 2F; Figure S3).

On the basis of the above findings, we postulated that our in vitro observation of differential effects of CST peptides on NO production via regulation of eNOS activity in HUVECs might be because of the differential interaction of CST peptides with ADRB2. Indeed, our computational analysis showed that by virtue of differences in secondary structures, CST-WT blocks the binding of the ligand to ADRB2 (by competing with it for the active site), whereas CST-364Ser binds at a site that keeps the agonist-binding pocket within ADRB2 intact (Figure 4C). Consistent with the computational prediction, competitive binding assays showed that although CST-WT was able to significantly displace the high-affinity β-adrenergic receptor ligand cyanopindolol, CST-364Ser failed to do the same even at high concentration (Figure 3B). Furthermore, the inhibition of agonist isoproterenol-stimulated increase in phospho-ERK levels by CST-WT (but not by CST-364Ser) in ADRB2 HEK-293 cells points toward an antiadrenergic role of the WT peptide but not the variant peptide (Figure 3C and 3D). This is consistent with a previous report that CST-WT lowers the phospho-ERK levels in Langendorff-perfused rat hearts.[21]

In contrast to the effective ability of CST-WT to bind to ADRB2, our computational studies show that CST peptides bind to the outer surface of the ADRB1 receptor and are thus incapable of blocking the agonist-binding pocket in the receptor. These observations are further supported by our competitive binding assays with ADRB1 (Figure S4B). Thus, the antiadrenergic role of CST-WT seems to be mediated primarily through the ADRB2 receptor and may underlie the differential BPs observed with the variants being expressed in patients.

Conclusions

We discovered a naturally occurring, common genetic variation, Gly364Ser, within the antihypertensive peptide CST, a proteolytic fragment of the prohormone chromogranin A that is expressed in secretory vesicles of endocrine, neuroendocrine, and neuronal cell types. The 364Ser allele showed association with elevated levels of SBP, DBP, and MAP in human subjects across 2 independent and ethnically/geographically distinct Indian populations. Corroborating these findings, the carriers of the 364Ser allele displayed enhanced risk for hypertension. This is on same lines of a recent Japanese study which found similar associations of the 364Ser allele with hypertension in their population. Genetic association studies of this chromogranin A locus with hypertension and other metabolic diseases need to be performed in additional ethnic populations to evaluate whether the results are of general importance across the overall world population as well. Our in cella and in silico analyses provided molecular/mechanistic underpinnings for the diminished effects of the CST-364Ser peptide (as compared with the CST-WT peptide) in the modulation of the endothelial NO pathway (via differential binding to ADRB2 and differential activation of ERK and eNOS phosphorylation) that might lead to an increased disease risk in carriers of the 364Ser allele. A schematic of our hypothesis/findings are presented in Figure 6. These results have implications for inter-individual variations in BP homeostasis and ultimately for pathogenesis of hypertension.

Perspectives

The neuroendocrine secretory granule protein chromogranin A is emerging as an important regulator of cardiovascular pathophysiology; it acts as precursor for several bioactive peptides including the antihypertensive and cardioprotective peptide CST. We discovered a nonsynonymous genetic variation (Gly364Ser that occurs in a large section of the worldwide human population) within the CST domain. The 364Ser allele was associated with profound elevated BP (up to ≈8 mm Hg SBP and ≈ 6 mm Hg DBP) and enhanced risk (by ≈48%) for hypertension in its carriers in several Asian populations. These findings contribute toward potential clinical use of functional genetic variations to predict the risk for hypertension and preventive intervention in asymptomatic patients for better management of cardiovascular disease burden.

Acknowledgments

We acknowledge all the individuals who voluntarily participated in this study. We thank the high-performance computational facility at Indian Institute of Technology Madras (IITM). We also thank Suvro Chatterjee, Anna University, Chennai, for his help. M. Kiranmayi and R. Kumaragurubaran thank Council of Scientific and Industrial Research for fellowship. P.K.R. Allu and D. Vishnuprabu received research fellowships from University Grants Commission. V.R. Chirasani, L. Subramanian, and S. Sharma would like to thank IITM, Department of Science and Technology, and Indian Council of Medical Research for fellowships, respectively.

Sources of Funding

This work was supported by grants BT/PR9546/MED/12/349/2007 and BT/PR12820/BRB/10/726/2009 from the Department of Biotechnology (DBT), Government of India. This work was also supported in part by grants SR/SO/HS-084/2013A from the Science and Engineering Research Board, BT/PR4820/MED/12/622/2013 from DBT, Government of India, and NIH RO1 HL HL089473.

Disclosures

None.

References

1. Kim T, Zhang CF, Sun Z, Wu H, Loh YP. Chromogranin A deficiency in transgenic mice leads to aberrant chromaffin granule biogenesis. *J Neurosci*. 2005;25:6958–6961. doi: 10.1523/JNEUROSCI.1058-05.2005.
2. O'Connor DT, Takiyyuddin MA, Printz MP, Dinh TQ, Barbosa JA, Rozansky DJ, Mahata SK, Wu H, Kennedy BP, Ziegler MG, Wright FA, Schlager G, Parmer RJ. Catecholamine storage vesicle protein expression in genetic hypertension. *Blood Press*. 1999;8:285–295.
3. Takiyyuddin MA, De Nicola L, Gabbai FB, Dinh TQ, Kennedy B, Ziegler MG, Sabban EL, Parmer RJ, O'Connor DT. Catecholamine secretory vesicles. Augmented chromogranins and amines in secondary hypertension. *Hypertension*. 1993;21:674–679.
4. Estensen ME, Hognestad A, Syversen U, Squire I, Ng L, Kjekshus J, Dickstein K, Omland T. Prognostic value of plasma chromogranin A levels in patients with complicated myocardial infarction. *Am Heart J*. 2006;152:927.e1–927.e6. doi: 10.1016/j.ahj.2006.05.008.

5. Jansson AM, Røsjø H, Omland T, Karlsson T, Hartford M, Flyvbjerg A, Caidahl K. Prognostic value of circulating chromogranin A levels in acute coronary syndromes. *Eur Heart J*. 2009;30:25–32. doi: 10.1093/eurheartj/ehn513.
6. Ceconi C, Ferrari R, Bachetti T, Opasich C, Volterrani M, Colombo B, Parrinello G, Corti A. Chromogranin A in heart failure; a novel neurohumoral factor and a predictor for mortality. *Eur Heart J*. 2002;23:967–974. doi: 10.1053/euhj.2001.2977.
7. Barbosa JA, Gill BM, Takiyyuddin MA, O'Connor DT. Chromogranin A: posttranslational modifications in secretory granules. *Endocrinology*. 1991;128:174–190. doi: 10.1210/endo-128-1-174.
8. Aardal S, Helle KB, Elsayed S, Reed RK, Serck-Hanssen G. Vasostatins, comprising the N-terminal domain of chromogranin A, suppress tension in isolated human blood vessel segments. *J Neuroendocrinol*. 1993;5:405–412.
9. Tatemoto K, Efendić S, Mutt V, Makk G, Feistner GJ, Barchas JD. Pancreastatin, a novel pancreatic peptide that inhibits insulin secretion. *Nature*. 1986;324:476–478. doi: 10.1038/324476a0.
10. Fasciotto BH, Trauss CA, Greeley GH, Cohn DV. Parastatin (porcine chromogranin A347-419), a novel chromogranin A-derived peptide, inhibits parathyroid cell secretion. *Endocrinology*. 1993;133:461–466. doi: 10.1210/endo.133.2.8344192.
11. Loh YP, Koshimizu H, Cawley NX, Tota B. Serpinins: role in granule biogenesis, inhibition of cell death and cardiac function. *Curr Med Chem*. 2012;19:4086–4092.
12. Simon JP, Bader MF, Aunis D. Secretion from chromaffin cells is controlled by chromogranin A-derived peptides. *Proc Natl Acad Sci USA*. 1988;85:1712–1716.
13. Mahata SK, O'Connor DT, Mahata M, Yoo SH, Taupenot L, Wu H, Gill BM, Parmer RJ. Novel autocrine feedback control of catecholamine release. A discrete chromogranin a fragment is a noncompetitive nicotinic cholinergic antagonist. *J Clin Invest*. 1997;100:1623–1633. doi: 10.1172/JCI119686.
14. Mahata SK, Mahata M, Wen G, Wong WB, Mahapatra NR, Hamilton BA, O'Connor DT. The catecholamine release-inhibitory "catestatin" fragment of chromogranin a: naturally occurring human variants with different potencies for multiple chromaffin cell nicotinic cholinergic responses. *Mol Pharmacol*. 2004;66:1180–1191. doi: 10.1124/mol.104.002139.
15. Sahu BS, Mohan J, Sahu G, Singh PK, Sonawane PJ, Sasi BK, Allu PK, Maji SK, Bera AK, Senapati S, Mahapatra NR. Molecular interactions of the physiological anti-hypertensive peptide catestatin with the neuronal nicotinic acetylcholine receptor. *J Cell Sci*. 2012;125(pt 9):2323–2337. doi: 10.1242/jcs.103176.
16. O'Connor DT, Kailasam MT, Kennedy BP, Ziegler MG, Yanaihara N, Parmer RJ. Early decline in the catecholamine release-inhibitory peptide catestatin in humans at genetic risk of hypertension. *J Hypertens*. 2002;20:1335–1345.
17. Mahapatra NR, O'Connor DT, Vaingankar SM, Hikim AP, Mahata M, Ray S, Staite E, Wu H, Gu Y, Dalton N, Kennedy BP, Ziegler MG, Ross J, Mahata SK. Hypertension from targeted ablation of chromogranin A can be rescued by the human ortholog. *J Clin Invest*. 2005;115:1942–1952. doi: 10.1172/JCI24354.
18. Wen G, Mahata SK, Cadman P, Mahata M, Ghosh S, Mahapatra NR, Rao F, Stridsberg M, Smith DW, Mahboubi P, Schork NJ, O'Connor DT, Hamilton BA. Both rare and common polymorphisms contribute functional variation at CHGA, a regulator of catecholamine physiology. *Am J Hum Genet*. 2004;74:197–207. doi: 10.1086/381399.
19. Sahu BS, Obbineni JM, Sahu G, Allu PK, Subramanian L, Sonawane PJ, Singh PK, Sasi BK, Senapati S, Maji SK, Bera AK, Gomathi BS, Mullasari AS, Mahapatra NR. Functional genetic variants of the catecholamine-release-inhibitory peptide catestatin in an Indian population: allele-specific effects on metabolic traits. *J Biol Chem*. 2012;287:43840–43852. doi: 10.1074/jbc.M112.407916.
20. Bassino E, Fornero S, Gallo MP, Ramella R, Mahata SK, Tota B, Levi R, Alloatti G. A novel catestatin-induced antiadrenergic mechanism triggered by the endothelial PI3K-eNOS pathway in the myocardium. *Cardiovasc Res*. 2011;91:617–624. doi: 10.1093/cvr/cvr129.
21. Angelone T, Quintieri AM, Brar BK, Limchaiyawat PT, Tota B, Mahata SK, Cerra MC. The antihypertensive chromogranin a peptide catestatin acts as a novel endocrine/paracrine modulator of cardiac inotropism and lusitropism. *Endocrinology*. 2008;149:4780–4793. doi: 10.1210/en.2008-0318.
22. Mazza R, Gattuso A, Mannarino C, Brar BK, Barbieri SF, Tota B, Mahata SK. Catestatin (chromogranin A344-364) is a novel cardiosuppressive agent: inhibition of isoproterenol and endothelin signaling in the frog heart. *Am J Physiol Heart Circ Physiol*. 2008;295:H113–H122. doi: 10.1152/ajpheart.00172.2008.
23. Imbrogno S, Garofalo F, Cerra MC, Mahata SK, Tota B. The catecholamine release-inhibitory peptide catestatin (chromogranin A344-363) modulates myocardial function in fish. *J Exp Biol*. 2010;213(pt 21):3636–3643. doi: 10.1242/jeb.045567.
24. Barrett JC, Fry B, Maller J, Daly MJ. Haploview: analysis and visualization of LD and haplotype maps. *Bioinformatics*. 2005;21:263–265. doi: 10.1093/bioinformatics/bth457.
25. Gauderman WJ. Sample size requirements for matched case-control studies of gene-environment interaction. *Stat Med*. 2002;21:35–50.
26. Giri H, Muthuramu I, Dhar M, Rathnakumar K, Ram U, Dixit M. Protein tyrosine phosphatase SHP2 mediates chronic insulin-induced endothelial inflammation. *Arterioscler Thromb Vasc Biol*. 2012;32:1943–1950. doi: 10.1161/ATVBAHA.111.239251.
27. Kesavan R, Potunuru UR, Nastasijević B, T A, Joksić G, Dixit M. Inhibition of vascular smooth muscle cell proliferation by Gentiana lutea root extracts. *PLoS One*. 2013;8:e61393. doi: 10.1371/journal.pone.0061393.
28. Noma T, Lemaire A, Naga Prasad SV, Barki-Harrington L, Tilley DG, Chen J, Le Corvoisier P, Violin JD, Wei H, Lefkowitz RJ, Rockman HA. Beta-arrestin-mediated beta1-adrenergic receptor transactivation of the EGFR confers cardioprotection. *J Clin Invest*. 2007;117:2445–2458. doi: 10.1172/JCI31901.
29. Naga Prasad SV, Barak LS, Rapacciuolo A, Caron MG, Rockman HA. Agonist-dependent recruitment of phosphoinositide 3-kinase to the membrane by beta-adrenergic receptor kinase 1. A role in receptor sequestration. *J Biol Chem*. 2001;276:18953–18959. doi: 10.1074/jbc.M102376200.
30. Vasudevan NT, Mohan ML, Gupta MK, Hussain AK, Naga Prasad SV. Inhibition of protein phosphatase 2A activity by PI3Kγ regulates β-adrenergic receptor function. *Mol Cell*. 2011;41:636–648. doi: 10.1016/j.molcel.2011.02.025.
31. Cherezov V, Rosenbaum DM, Hanson MA, Rasmussen SG, Thian FS, Kobilka TS, Choi HJ, Kuhn P, Weis WI, Kobilka BK, Stevens RC. High-resolution crystal structure of an engineered human beta2-adrenergic G protein-coupled receptor. *Science*. 2007;318:1258–1265. doi: 10.1126/science.1150577.
32. Allu PK, Chirasani VR, Ghosh D, Mani A, Bera AK, Maji SK, Senapati S, Mullasari AS, Mahapatra NR. Naturally occurring variants of the dysglycemic peptide pancreastatin: differential potencies for multiple cellular functions and structure-function correlation. *J Biol Chem*. 2014;289:4455–4469. doi: 10.1074/jbc.M113.520916.
33. Webb B, Sali A. Comparative protein structure modeling using MODELLER. *Curr Protoc Bioinformatics*. 2014;47:5.6.1–5.632. doi: 10.1002/0471250953.bi0506s47.
34. Pierce BG, Wiehe K, Hwang H, Kim BH, Vreven T, Weng Z. ZDOCK server: interactive docking prediction of protein-protein complexes and symmetric multimers. *Bioinformatics*. 2014;30:1771–1773. doi: 10.1093/bioinformatics/btu097.
35. Humphrey W, Dalke A, Schulten K. VMD: visual molecular dynamics. *J Mol Graph*. 1996;14:33–38, 27.
36. de Beer TA, Berka K, Thornton JM, Laskowski RA. PDBsum additions. *Nucleic Acids Res*. 2014;42(Database issue):D292–D296. doi: 10.1093/nar/gkt940.
37. Laskowski RA, Swindells MB. LigPlot+: multiple ligand-protein interaction diagrams for drug discovery. *J Chem Inf Model*. 2011;51:2778–2786. doi: 10.1021/ci200227u.
38. Cui JS, Hopper JL, Harrap SB. Antihypertensive treatments obscure familial contributions to blood pressure variation. *Hypertension*. 2003;41:207–210.
39. Rao F, Wen G, Gayen JR, et al. Catecholamine release-inhibitory peptide catestatin (chromogranin A(352-372)): naturally occurring amino acid variant Gly364Ser causes profound changes in human autonomic activity and alters risk for hypertension. *Circulation*. 2007;115:2271–2281. doi: 10.1161/CIRCULATIONAHA.106.628859.
40. Taupenot L, Harper KL, O'Connor DT. The chromogranin-secretogranin family. *N Engl J Med*. 2003;348:1134–1149. doi: 10.1056/NEJMra021405.
41. Queen LR, Ferro A. Beta-adrenergic receptors and nitric oxide generation in the cardiovascular system. *Cell Mol Life Sci*. 2006;63:1070–1083. doi: 10.1007/s00018-005-5451-2.
42. Morris GM, Huey R, Lindstrom W, Sanner MF, Belew RK, Goodsell DS, Olson AJ. AutoDock4 and AutoDockTools4: automated docking with selective receptor flexibility. *J Comput Chem*. 2009;30:2785–2791. doi: 10.1002/jcc.21256.

43. Miller-Gallacher JL, Nehmé R, Warne T, Edwards PC, Schertler GF, Leslie AG, Tate CG. The 2.1 Å resolution structure of cyanopindolol-bound β1-adrenoceptor identifies an intramembrane Na+ ion that stabilises the ligand-free receptor. *PLoS One*. 2014;9:e92727. doi: 10.1371/journal.pone.0092727.
44. Adzhubei IA, Schmidt S, Peshkin L, Ramensky VE, Gerasimova A, Bork P, Kondrashov AS, Sunyaev SR. A method and server for predicting damaging missense mutations. *Nat Methods*. 2010;7:248–249. doi: 10.1038/nmeth0410-248.
45. Mahapatra NR. Catestatin is a novel endogenous peptide that regulates cardiac function and blood pressure. *Cardiovasc Res*. 2008;80:330–338. doi: 10.1093/cvr/cvn155.
46. Mazza R, Tota B, Gattuso A. Cardio-vascular activity of catestatin: interlocking the puzzle pieces. *Curr Med Chem*. 2015;22:292–304.
47. Sahu BS, Sonawane PJ, Mahapatra NR. Chromogranin A: a novel susceptibility gene for essential hypertension. *Cell Mol Life Sci*. 2010;67:861–874. doi: 10.1007/s00018-009-0208-y.
48. Gayen JR, Gu Y, O'Connor DT, Mahata SK. Global disturbances in autonomic function yield cardiovascular instability and hypertension in the chromogranin a null mouse. *Endocrinology*. 2009;150:5027–5035. doi: 10.1210/en.2009-0429.
49. Kennedy BP, Mahata SK, O'Connor DT, Ziegler MG. Mechanism of cardiovascular actions of the chromogranin A fragment catestatin in vivo. *Peptides*. 1998;19:1241–1248.
50. Fung MM, Salem RM, Mehtani P, Thomas B, Lu CF, Perez B, Rao F, Stridsberg M, Ziegler MG, Mahata SK, O'Connor DT. Direct vasoactive effects of the chromogranin A (CHGA) peptide catestatin in humans in vivo. *Clin Exp Hypertens*. 2010;32:278–287. doi: 10.3109/10641960903265246.
51. Gaede AH, Pilowsky PM. Catestatin in rat RVLM is sympathoexcitatory, increases barosensitivity, and attenuates chemosensitivity and the somatosympathetic reflex. *Am J Physiol Regul Integr Comp Physiol*. 2010;299:R1538–R1545. doi: 10.1152/ajpregu.00335.2010.
52. Gaede AH, Pilowsky PM. Catestatin, a chromogranin A-derived peptide, is sympathoinhibitory and attenuates sympathetic barosensitivity and the chemoreflex in rat CVLM. *Am J Physiol Regul Integr Comp Physiol*. 2012;302:R365–R372. doi: 10.1152/ajpregu.00409.2011.
53. Dorajoo R, Blakemore AI, Sim X, Ong RT, Ng DP, Seielstad M, Wong TY, Saw SM, Froguel P, Liu J, Tai ES. Replication of 13 obesity loci among Singaporean Chinese, Malay and Asian-Indian populations. *Int J Obes (Lond)*. 2012;36:159–163. doi: 10.1038/ijo.2011.86.
54. Ntzani EE, Liberopoulos G, Manolio TA, Ioannidis JP. Consistency of genome-wide associations across major ancestral groups. *Hum Genet*. 2012;131:1057–1071. doi: 10.1007/s00439-011-1124-4.
55. Carlson CS, Matise TC, North KE, et al; PAGE Consortium. Generalization and dilution of association results from European GWAS in populations of non-European ancestry: the PAGE study. *PLoS Biol*. 2013;11:e1001661. doi: 10.1371/journal.pbio.1001661.
56. Hiura Y, Tabara Y, Kokubo Y, Okamura T, Miki T, Tomoike H, Iwai N. A genome-wide association study of hypertension-related phenotypes in a Japanese population. *Circ J*. 2010;74:2353–2359.
57. Guo Y, Tomlinson B, Chu T, Fang YJ, Gui H, Tang CS, Yip BH, Cherny SS, Hur YM, Sham PC, Lam TH, Thomas NG. A genome-wide linkage and association scan reveals novel loci for hypertension and blood pressure traits. *PLoS One*. 2012;7:e31489. doi: 10.1371/journal.pone.0031489.
58. Takiyyuddin MA, Parmer RJ, Kailasam MT, Cervenka JH, Kennedy B, Ziegler MG, Lin MC, Li J, Grim CE, Wright FA. Chromogranin A in human hypertension. Influence of heredity. *Hypertension*. 1995;26:213–220.
59. Choi Y, Miura M, Nakata Y, et al. A common genetic variant of the chromogranin A-derived peptide catestatin is associated with atherogenesis and hypertension in a Japanese population. *Endocr J*. 2015;62:797–804. doi: 10.1507/endocrj.EJ14-0471.
60. Radha V, Vimaleswaran KS, Babu HN, Abate N, Chandalia M, Satija P, Grundy SM, Ghosh S, Majumder PP, Deepa R, Rao SM, Mohan V. Role of genetic polymorphism peroxisome proliferator-activated receptor-gamma2 Pro12Ala on ethnic susceptibility to diabetes in South-Asian and Caucasian subjects: evidence for heterogeneity. *Diabetes Care*. 2006;29:1046–1051. doi: 10.2337/diacare.2951046.
61. Lüscher TF, Diederich D, Weber E, Vanhoutte PM, Bühler FR. Endothelium-dependent responses in carotid and renal arteries of normotensive and hypertensive rats. *Hypertension*. 1988;11(6 pt 2):573–578.
62. Fu-Xiang D, Jameson M, Skopec J, Diederich A, Diederich D. Endothelial dysfunction of resistance arteries of spontaneously hypertensive rats. *J Cardiovasc Pharmacol*. 1992;20(suppl 12):S190–S192.
63. Panza JA, Casino PR, Kilcoyne CM, Quyyumi AA. Role of endothelium-derived nitric oxide in the abnormal endothelium-dependent vascular relaxation of patients with essential hypertension. *Circulation*. 1993;87:1468–1474.
64. Panza JA, García CE, Kilcoyne CM, Quyyumi AA, Cannon RO, 3rd. Impaired endothelium-dependent vasodilation in patients with essential hypertension. Evidence that nitric oxide abnormality is not localized to a single signal transduction pathway. *Circulation*. 1995;91:1732–1738.
65. Gayen JR, Zhang K, RamachandraRao SP, Mahata M, Chen Y, Kim HS, Naviaux RK, Sharma K, Mahata SK, O'Connor DT. Role of reactive oxygen species in hyperadrenergic hypertension: biochemical, physiological, and pharmacological evidence from targeted ablation of the chromogranin a (Chga) gene. *Circ Cardiovasc Genet*. 2010;3:414–425. doi: 10.1161/CIRCGENETICS.109.924050.
66. Mazza R, Pasqua T, Gattuso A. Cardiac heterometric response: the interplay between Catestatin and nitric oxide deciphered by the frog heart. *Nitric Oxide*. 2012;27:40–49. doi: 10.1016/j.niox.2012.04.003.
67. Michell BJ, Chen Zp, Tiganis T, Stapleton D, Katsis F, Power DA, Sim AT, Kemp BE. Coordinated control of endothelial nitric-oxide synthase phosphorylation by protein kinase C and the cAMP-dependent protein kinase. *J Biol Chem*. 2001;276:17625–17628. doi: 10.1074/jbc.C100122200.
68. Butt E, Bernhardt M, Smolenski A, Kotsonis P, Fröhlich LG, Sickmann A, Meyer HE, Lohmann SM, Schmidt HH. Endothelial nitric-oxide synthase (type III) is activated and becomes calcium independent upon phosphorylation by cyclic nucleotide-dependent protein kinases. *J Biol Chem*. 2000;275:5179–5187.
69. Ferro A, Queen LR, Priest RM, Xu B, Ritter JM, Poston L, Ward JP. Activation of nitric oxide synthase by beta 2-adrenoceptors in human umbilical vein endothelium *in vitro*. *Br J Pharmacol*. 1999;126:1872–1880. doi: 10.1038/sj.bjp.0702512.
70. Yao K, Xu B, Liu YP, Ferro A. Effects of beta-adrenoceptor stimulation on endothelial nitric-oxide synthase phosphorylation of human umbilical vein endothelial cells. *Acta Pharmacol Sin*. 2003;24:219–224.

Novelty and Significance

What Is New?

- This is the first study that analyzes the association of the Gly364Ser variant in the antihypertensive peptide catestatin with the risk for hypertension in independent Asian populations.
- This study provides evidence for the direct interaction of catestatin peptides with β-2 adrenergic receptor for the first time to our knowledge.

What Is Relevant?

- This study identifies a novel blood pressure–regulating locus that seems to play an important role to alter the risk for hypertension in several Asian populations.

Summary

Directionally concordant replication of the association of catestatin 364Ser variant allele with elevated blood pressure in independent human populations suggests a causal role for this genetic variant. Consistently, the 364Ser allele enhanced the risk for hypertension in these study populations. Moreover, our receptor–peptide interaction studies provided evidence for differential interactions of the wild-type and variant catestatin peptides with β-2 adrenergic receptor that might be responsible for the altered risk for hypertension in their carriers.

Catestatin Gly364Ser Variant Alters Systemic Blood Pressure and the Risk for Hypertension in Human Populations via Endothelial Nitric Oxide Pathway

Malapaka Kiranmayi, Venkat R. Chirasani, Prasanna K.R. Allu, Lakshmi Subramanian, Elizabeth E. Martelli, Bhavani S. Sahu, Durairajpandian Vishnuprabu, Rathnakumar Kumaragurubaran, Saurabh Sharma, Dhanasekaran Bodhini, Madhulika Dixit, Arasambattu K. Munirajan, Madhu Khullar, Venkatesan Radha, Viswanathan Mohan, Ajit S. Mullasari, Sathyamangla V. Naga Prasad, Sanjib Senapati and Nitish R. Mahapatra

Hypertension. 2016;68:334-347; originally published online June 20, 2016;
doi: 10.1161/HYPERTENSIONAHA.116.06568
Hypertension is published by the American Heart Association, 7272 Greenville Avenue, Dallas, TX 75231

Print ISSN: 0194-911X. Online ISSN: 1524-4563

SUPPLEMENTARY INFORMATION

CATESTATIN GLY364SER VARIANT ALTERS SYSTEMIC BLOOD PRESSURE AND THE RISK FOR HYPERTENSION IN HUMAN POPULATIONS VIA ENDOTHELIAL NO PATHWAY

Malapaka Kiranmayi[1], Venkat R Chirasani[1], Prasanna K R Allu[1,7], Lakshmi Subramanian[1], Elizabeth E Martelli[2], Bhavani S Sahu[1,8], Durairajpandian Vishnuprabu[3], Rathnakumar Kumaragurubaran[1], Saurabh Sharma[4], Dhanasekaran Bodhini[5], Madhulika Dixit[1], Arasambattu K Munirajan[3], Madhu Khullar[4], Venkatesan Radha[5], Viswanathan Mohan[5], Ajit S Mullasari[6], Sathyamangla V Naga Prasad[2], Sanjib Senapati[1], Nitish R Mahapatra[1,*]

from the

[1]Department of Biotechnology, Bhupat and Jyoti Mehta School of Biosciences, Indian Institute of Technology Madras, Chennai, Tamil Nadu, India

[2]Department of Molecular Cardiology, Lerner Research Institute, Cleveland Clinic, Ohio, USA

[3]Department of Genetics, University of Madras, Chennai, Tamil Nadu, India

[4]Department of Experimental Medicine and Biotechnology, Postgraduate Institute of Medical Education and Research, Chandigarh, India

[5]Department of Molecular Genetics, Madras Diabetes Research Foundation, Chennai, Tamil Nadu, India

[6]Institute of Cardiovascular Diseases, Madras Medical Mission, Chennai, Tamil Nadu, India

[7]Deptartment of Medicine, University of California San Francisco, California, USA

[8]Department of Clinical Biochemistry, University of Cambridge, Cambridge, UK

DETAILED METHODS

Human subjects and study design for primary study (Chennai population)

The present case-control study enrolled a total of 3200 unrelated human subjects, comprising 1705 hypertensive/diabetic cases (with no history of cancer/kidney disease), 519 coronary artery disease (CAD) samples and 976 controls (with no history of hypertension/diabetes/cancer/kidney disease). The subjects were recruited from the urban cosmopolitan population of Chennai, the fourth largest city in India, at three independent centres - hypertensive/diabetic cases from The Institute of Cardiovascular Diseases, Madras Medical Mission (MMM) and Madras Diabetes Research Foundation (MDRF) and CAD samples from Madras Medical College (MMC). At MMM, peripheral venipuncture was carried out to collect blood samples. These samples were stored in EDTA-containing tubes for the isolation of genomic DNA at a later time. Plasma samples were also collected, aliquoted, and stored at -80°C for assaying various biochemical parameters. At MDRF, the samples were collected in the form of genomic DNA. At MMC, the samples were collected in the form of genomic DNA. Each subject gave informed, written consent for the use of their sample in this study. The study was approved by the Institute Ethics Committees at MMM, MDRF, MMC and Indian Institute of Technology Madras. Data was also collected regarding the demographic parameters (age, sex), physical parameters (height, weight, and body mass index [BMI]), physiological parameters (systolic blood pressure (SBP), diastolic blood pressure (DBP), mean arterial pressure (MAP), heart rate (HR), left ventricular dimension at end of systole (LVIDs) and left ventricular dimension at end of diastole (LVIDd)), biochemical parameters (hemoglobin, sodium, potassium, urea, creatinine, blood sugar, total cholesterol [TC], triglycerides [TGL], insulin, HOMA-IR index and HbA1c) and medical history (current medication, family history of cardiovascular and renal disease states) of the cases and

controls. Blood pressure was measured on the sitting position by experienced nursing staff using a brachial oscillometric cuff, and triplicate values were averaged. Supplementary Table S2 describes the demographic, physiological and biochemical parameters of the study subjects by case, control status. In the Chennai DM/HTN/controls population, the average age of the subjects was ~43 years. Out of the 1705 cases, 721 were essential hypertensives, 472 were diabetic and 512 had both hypertension and diabetes. 74% of the hypertensive subjects were on antihypertensive medications such as angiotensin II receptor blocker, angiotensin convertase enzyme inhibitors, beta blockers and calcium channel blockers. In case of diabetic subjects, 29% were receiving diabetic medications such as oral hypoglycemic agents and insulin. The diabetic/hypertensive cases differed from the controls in terms of BMI ($p<0.001$), SBP ($p<0.001$), DBP ($p<0.001$), MAP ($p<0.001$), LVIDs ($p=0.001$), blood sugar ($p<0.001$), TC ($p<0.001$), TGL ($p<0.001$) and fasting blood sugar (FBS) insulin ($p<0.001$). The CAD cases had an average age of 51 years.

Human subjects and study design for replication population (Chandigarh)

To validate our primary study in a geographically separated population, we studied 760 unrelated human subjects from North India (Chandigarh). The human subjects were recruited at the Post Graduate Institute of Medical Education and Research (PGIMER), Chandigarh, and consisted of 401 hypertensive cases (with no history of cancer/kidney disease) and 359 normotensive controls (with no history of hypertension/diabetes/cancer/kidney disease). Supplementary Table S3 describes the demographic, physiological and biochemical parameters of the study subjects by case, control status. The samples were obtained in the form of genomic DNA for all the 760 human subjects. All subjects were informed of the purpose of the study and their written consent was obtained. The study was approved by the Institute Ethics Committee at PGIMER. Data regarding the demographic parameters (age, sex), physical parameters (BMI), physiological

parameters (pre-treatment SBP, DBP, and MAP), biochemical parameters (hemoglobin, sodium, potassium, urea, creatinine, blood sugar, TC, TGL) and current medication of the subjects was collected. In the Chandigarh population, the average age of the subjects was ~53 years. The hypertensive cases differed from the controls in terms of SBP ($p<0.001$), DBP ($p<0.001$) and MAP ($p<0.001$).

Genotyping of the CST 364Ser variant

Sanger's sequencing: Out of the 3960 samples, 1763 samples were genotyped using the PCR-purification-Sanger's sequencing protocol as described previously [1]. Genomic DNA was prepared from the EDTA-anti-coagulated blood samples according to the manufacturer's instructions using the FlexiGene DNA kit (Qiagen, USA). With this genomic DNA as template, forward primer: 5'-GAGTGGCAGAGACTGGGAAAATG-3' and reverse primer: 5'-ACAGAGCTGGCTCCCGCCC-3' were used to PCR amplify the exon-7 region of *CHGA*. The PCR amplicons were purified using QIAquick PCR purification columns (Qiagen, USA) and sequenced using an Applied Biosystems 3130 Genetic Analyzer (USA). All the samples were sequenced initially using the forward primer (as described above). Each chromatogram was manually checked for the confirmation of the genetic variants. In case of any ambiguity regarding a polymorphism, the sample was re-sequenced using the reverse primer (as described above).

Taqman® assay: The remaining 2197 samples were genotyped using the Taqman® assay. Taqman® SNP genotyping assay was performed in a 384 well microAmp PCR plate (Applied Biosystems [ABI], USA). The 5 µl PCR comprised of 10 ng genomic DNA and 2.5 µl of 2X TaqMan® Universal PCR master mix No UNG and 0.125 µl of 40X TaqMan® SNP Genotyping assay mix (Probes and Primers) (ABI, USA). Absolute Quantification was performed according to the manufacturer's recommendation (2 min at 50°C, 10 min at 95°C followed by 15 sec at

92°C and 60 sec at 60°C for 40 cycles) and Allelic discrimination with endpoint detection of fluorescence was performed in ABI 7900HT real-time PCR system (ABI, USA). Non-template controls and positive controls (known homozygous variants) were routinely added in each reaction. Genotype calls were selected by 95% quality calls using Sequence Detection Software (SDS) (ABI, USA).

Estimation of biochemical parameters

Standard biochemical assays were used to measure biochemical parameters such as glucose (random blood sugar, fasting blood sugar, and post-glucose blood sugar), total cholesterol, triglycerides, urea, creatinine, hemoglobin, sodium and potassium levels in the plasma. The blood pressure readings are an average of triplicate values recorded in the sitting position using a brachial oscillometric cuff by experienced nursing staff.

Data representation and statistical analysis

The experimental data results and the human study phenotypic parameters are expressed as mean ± SE. Allele frequencies were estimated by gene counting. A Pearson's χ^2 test was employed to compare the distribution of the genotypes. Statistical analysis was carried out using the Statistical Package for Social Sciences (SPSS) Version 21.0. To identify the risk of the genotype for any of the disease conditions, logistic regression analysis was carried out using the disease condition (DM, HTN, CAD, metabolic disease) as the dependent variable and the genotypes (risk factors) and age, sex and BMI (covariates adjusted in the analysis) as the independent variables. Outliers with abnormal values for any of the parameters were removed by quartile analysis. To evaluate the association of the variant allele with the phenotypic parameters, the Levene's test for equality of variance and t-test for equality of means were performed with the homozygotes for the major allele (wild-type CST-364Gly/Gly) individuals coded as 0 and the heterozygotes as well as homozygotes for the minor allele (CST-364Gly/Ser and CST-364Ser/Ser, respectively) coded as

1. Owing to their small numbers (n=18) in the overall population, the homozygous variant individuals were grouped with the heterozygous variant individuals. The overall population was further divided into different disease groups (all cases, only hypertensives, only diabetics, subjects with both hypertension and diabetes, CAD, controls) and statistical analysis was carried out among these groups as well to identify any allele-specific associations with the various disease conditions. Analysis of covariance (ANCOVA) was also carried out in a univariate general linear model after adjusting for age as a covariate. Haploview 4.2 was used for linkage disequilibrium analysis. Deviations from the Hardy-Weinberg equilibrium were calculated using the online calculator provided by Tufts University, Boston, MA: http://www.tufts.edu/ mcourt01/Documents/ Court%20lab%20-%20HW%20calculator.xls. A p value of <0.05 was chosen as statistically significant. The power of the study was calculated using Quanto version 1.2.4. Meta-analysis was carried out using the OpenMeta[Analyst] software (www.cebm.brown.edu/open_meta/).

Synthesis of CST peptides

The CST wild type (CST-WT, SSMKLSFRARAYGFRGPGPQL) and CST-364Ser variant (CST-Ser364, SSMKLSFRARAY**S**FRGPGPQL) peptides were synthesized by solid phase method and purified to 95% homogeneity as described previously [1]. The purity and molecular weights of these peptides were verified by analytical high performance liquid chromatography and mass spectrometry.

Human umbilical vein endothelial cells (HUVECs) isolation and culture conditions

Experimental procedures involving umbilical cords were reviewed and approved by the IIT Madras institutional ethics committee in accordance with Declaration of Helsinki revised in 2000 (reference number: IITM IEC No. 2009024). HUVECs were isolated from umbilical cords by

digestion with collagenase as described previously [2]. HUVECs in passage 2 were used for all the experiments. Cells were cultured in MCDB131 medium (from HiMedia) supplemented with EGM™ SingleQuots™ (Lonza, USA). Isolated cells were seeded onto fibronectin coated T-25 flasks and grown to confluence with 10% Fetal Bovine Serum (FBS). Cells were sub-cultured for experimental conditions either in 6-well or 24 well fibronectin-coated tissue culture dishes.

Measurement of nitric oxide (NO) levels in cultured HUVECs

NO levels in HUVECs were measured by 4, 5-Diaminofluorescein diacetate (DAF-2 DA) method as described previously [3]. HUVECs were first seeded in 24-well plates and on reaching 60-70% confluence (i.e., 24 hours after seeding), cells were serum-starved for 12 hours and then treated with different doses of CST-WT or CST-364Ser for 20 min at 37°C. The peptides were prepared in serum-free media. After the 20 minute treatment, serum-free media containing the peptides was removed and the cells were incubated with 10 µmol/L DAF-2 DA (Sigma-Aldrich) and 1.0 mmol/L L-Arginine (nitric oxide synthases [NOS] substrate; Sigma-Aldrich) in serum-free media for 20 min at 37°C. The cells were then washed twice with phosphate buffer saline (PBS) and the fluorescence was detected by a Nikon-Ti Eclipse fluorescence microscope (Japan) with excitation wavelength of 485 nm and emission wavelength of 530 nm. For each condition, three fields were captured. The NO index was arrived at by measuring the mean fluorescence intensity for n=50 cells/field using ImageJ software. The experiments were repeated at least 3 times. For the antagonists experiments, the cells were treated with 300 nmol/L CGP 20712 and 100 nmol/L ICI 118551 for 20 min at 37°C before treatment with the peptides. The antagonists were prepared in serum-free media.

ADRB1/2 HEK-293 cells culture and treatment

Human embryonic kidney (HEK) 293 cells that stably over-express ADRB1/2 (ADRB1/2 HEK-293) were used to test whether CST peptides bind to ADRB1/2. ADRB1/2 HEK-293 cells were maintained in minimal essential medium (MEM) supplemented with 10% FBS and penicillin-streptomycin at 37°C. Cells were seeded at a density of ~1 x 10^6 cells/100 mm and were subjected to treatments at 60-80% confluence. At 60-80% confluence cells were serum starved in MEM at 37°C for 4 hours. To test whether CST treatment alters ADRB1/2 agonist responses, ADRB1/2 HEK-293 cells were pre-incubated with CST-WT and CST-364Ser peptides (10 μmol/L) for 45 minutes followed by ADRB agonist isoproterenol (10 μmol/L) for 0, 5 and 10 minutes.

Isolation of ADRB1/2-expressing plasma membranes

Purification of plasma membrane was performed as described previously [4, 5]. Plasma membranes from control HEK-293 and ADRB1/2 HEK-293 cells were isolated by briefly homogenizing cells in ice-cold lysis buffer containing 5 mmol/L Tris-HCl (pH 7.5), 5 mmol/L EDTA, 1 mmol/L PMSF, and 2 μg/ml Leupeptin and Aprotinin. Cell debris/nuclei were removed by centrifugation at 1000 x g for 5 minutes at 4°C. Supernatant was transferred to a new tube and subjected to centrifugation at 37,000 x g for 30 minutes at 4°C. The pellet containing plasma membrane was re-suspended in 75 mmol/L Tris-HCl (pH 7.5), 2 mmol/L EDTA, 12.5 mmol/L $MgCl_2$ and was used for ligand binding assays.

Radio-ligand binding and competition binding assays

To test for the level of ADRB1/2 expression in ADRB1/2 HEK-293 cells, [^{125}I]-cyanopindolol saturation radio-ligand binding was performed on the plasma membranes isolated from control HEK-293 and ADRB1/2 HEK-293 cells as described previously [4, 5]. Briefly, 20 μg of plasma membranes were incubated with saturating concentrations of cyanopindolol (250 pmol/L) alone

or along with 100 μmol/L Propranolol. Propranolol was used for determining non-specific binding. The samples were incubated at 37°C for 1 hour, harvested using BRANDEL cell harvester system (BRANDEL, USA) on to a GF/C filter paper and the bound ligand ascertained using BECKMAN LS6000IC (BECKMAN, USA) gamma counter.

An indirect, competitive ligand binding assay was performed where the binding of CST peptides, CST-WT and CST-364Ser, to the ADRB1/2 over-expressing membrane surface in ADRB1/2-HEK-293 cells was measured in terms of their ability to displace the bound high-affinity radio-labeled ligand, cyanopindolol. 20 μg of plasma membranes were incubated with saturating concentrations of cyanopindolol and increasing concentrations of the CST peptides (from 10 pmol/L to 1 mmol/L). Following incubation at 37°C for 1 hour, samples were harvested using BRANDEL cell harvester system (BRANDEL, USA) and the bound ligand was determined using the BECKMAN LS6000IC (BECKMAN, USA) gamma counter.

Western immunoblotting

Activation of ADRB1/2 in HEK-293 cells was assessed in terms of activation of extracellular regulated kinase (ERK) by performing immunoblotting and detection of phospho-ERK as described previously [6]. Cells were harvested in NP40 lysis buffer containing 20 mmol/L Tris (pH 7.4), 137 mmol/L NaCl, 1% NP-40, 1 mmol/L PMSF, 20% Glycerol, 10 mmol/L NaF, 1 mmol/L Sodium Orthovanadate, 2μg/ml Leupeptin and Aprotinin. The lysates were cleared by centrifugation at 12000 x g for 15 min at 4°C. 70-120 μg of the supernatant cell lysate was resolved by SDS-PAGE and transferred onto PVDF membranes (BIO-RAD) for western immunoblotting analysis. The membranes were blocked with 5% BSA and incubated with anti-phospho ERK antibody at 1:1000 dilution to recognize activated ERK. Following primary antibody incubation, appropriate secondary antibody (1:3000) was used and detection was

carried out using enhanced chemiluminescence. Quantitative densitometric analysis was carried out using the NIH Image J software.

Activation of eNOS in HUVECs with/without treatment with CST peptides was assessed by western blotting and detection of Ser^{1177} phosphorylated eNOS. HUVECs were first seeded in 12-well plates and on reaching 60-70% confluence (i.e., 24 hours after seeding), cells were serum-starved for 12 hours and then treated with 1 nmol/L CST-WT or CST-364Ser for 20 min at 37°C. Cells were harvested in RIPA lysis buffer containing 50 mmol/L Tris (pH 8.0), 150 mmol/L NaCl, 1% Triton X-100, 1x Protease Inhibitor Cocktail, 0.1% SDS. The lysates were cleared by centrifugation at 12000 x g for 15 min at 4°C. 30-40 μg of the supernatant cell lysate was resolved by SDS-PAGE and transferred onto PVDF membrane (BIO-RAD) for western immunoblotting analysis. The membrane was blocked with 5% BSA for Ser^{1177} and 3% BSA for total eNOS at room temperature for an hour. The membrane was then incubated with anti-phospho Ser^{1177} eNOS antibody (Cell Signaling, USA) and anti-total eNOS antibody (Santa Cruz, USA) at 1:1000 dilutions to recognize phospo-eNOS and total eNOS. Following primary antibody incubation, appropriate secondary antibody (1:5000) was used and detection was carried out using enhanced chemiluminescence. Quantitative densitometric analysis was carried out using the NIH Image J software.

Modelling of the ADRB1 and ADRB2 receptors and the CST-WT and CST-364Ser peptide structures

The crystal structure of ADRB2 with resolution 2.4 Å was obtained from protein data bank (PDB ID:2RH1) [7]. The bound ligands and crystal water were stripped out from the protein structure and subsequently energy minimized to obtain a more sophisticated model of ADRB2 for protein-protein docking. The structure of ADRB1 was modelled based on the structure of ADRB2 as a

template. The regions in ADRB1 with poor structural homology were excluded from the structure during refinement.

The structure of 21-mer human wild-type CST (CST-WT) has already been determined by NMR (PDB ID:1LV4) [8]. However, the absence of any secondary structural elements in the NMR structure called for a more detailed elucidation of the peptide's conformation. In this work, we generated 3D structures of CST-WT and its variant CST-364Ser following a similar protocol as proposed earlier [9]. The NMR structure of CST was downloaded from protein data bank and subjected to short energy minimization for optimal positioning of the side chains. Residue Gly364 in the CST structure was mutated to 364Ser using Modeller 9v13 [10] and a short energy minimization was imposed to optimize the side chain positions. The final refinements for CST-WT as well as CST-364Ser were carried out by molecular dynamics (MD) simulations. The minimized structures were subsequently subjected to 300 nanoseconds explicit water MD simulations to generate an ensemble of both CST-WT and CST-364Ser conformations.

MD simulations methodology

All the simulations were performed using Gromacs-4.5.5 simulation package [11] and AMBER99SB force-field parameters [12]. First, the system was energy minimized using conjugate gradient and steepest descent algorithms, each with 1000 steps. The energy-minimized protein structure was subsequently solvated in a cubic periodic box with about 2400 explicit water molecules. In MD simulations, an initial drift is anticipated as the peptide residues diminish any unfavorable interactions and the solvent molecules relax around them. Hence, the structural analyses of the peptides were executed on the last 25 ns simulation data. TIP3P model was used to describe the water molecules. A salt concentration of 0.15 M was maintained with appropriate number of Na^+ and Cl^- ions to mimic the physiological ionic strength. The solvated system was again energy minimized and subsequently heated to 310 K. The system was equilibrated in NPT

ensemble at 1 atm and 310 K for about 10 ns, by when the solvent density, system temperature reached a plateau. This followed a production phase of 300 ns, on which all analyses were performed. Long-range electrostatic interactions were described using Particle Mesh Ewald sum technique [13] with a real space cut-off of 1.0 nm and SHAKE algorithm [14] was used to constrain all bonds involving hydrogen atoms.

Protein-protein docking of CST-WT and CST-364Ser with ADRB1/2 receptors

Protein-protein docking of CST peptides on ADRB1/2 was performed using ZDOCK docking algorithm [15] to locate the probable binding sites of CST peptides in ADRB1/2 structure. ZDOCK performs efficient global docking search on a 3D grid by using Fast Fourier Transform algorithm and scores docked complexes based on combination of shape complementarity, electrostatics and statistical potential terms [16]. During molecular docking, CST peptides were allowed to search the extra cellular region of the ADRB1/2 receptors to identify the best binding location. ZDOCK predicted 100 binding modes of CST peptides with ADRB1/2, which were ranked according to ZDOCK docking score. The best docked complex was then identified based on this score.

All the structural figures were rendered using Visual Molecular Dynamics (VMD) [17]. The ADRB2-CST interactions were identified using PDBsum [18] and cyanopindolol-ADRB2 interactions were identified using LigPlot+ [19].

REFERENCES FOR SUPPLEMENTARY INFORMATION

1. Sahu BS, Obbineni JM, Sahu G, Allu PK, Subramanian L, Sonawane PJ, Singh PK, Sasi BK, Senapati S, Maji SK, Bera AK, Gomathi BS, Mullasari AS, Mahapatra NR. Functional genetic variants of the catecholamine-release-inhibitory peptide catestatin in an indian population: Allele-specific effects on metabolic traits. *J Biol Chem*. 2012;287:43840-43852.
2. Giri H, Muthuramu I, Dhar M, Rathnakumar K, Ram U, Dixit M. Protein tyrosine phosphatase shp2 mediates chronic insulin-induced endothelial inflammation. *Arterioscler Thromb Vasc Biol*. 2012;32:1943-1950.
3. Kesavan R, Potunuru UR, Nastasijevic B, T A, Joksic G, Dixit M. Inhibition of vascular smooth muscle cell proliferation by gentiana lutea root extracts. *PLoS One*. 2013;8:e61393.
4. Naga Prasad SV, Barak LS, Rapacciuolo A, Caron MG, Rockman HA. Agonist-dependent recruitment of phosphoinositide 3-kinase to the membrane by beta-adrenergic receptor kinase 1. A role in receptor sequestration. *J Biol Chem*. 2001;276:18953-18959.
5. Vasudevan NT, Mohan ML, Gupta MK, Hussain AK, Naga Prasad SV. Inhibition of protein phosphatase 2a activity by pi3kgamma regulates beta-adrenergic receptor function. *Mol Cell*. 2011;41:636-648.
6. Noma T, Lemaire A, Naga Prasad SV, Barki-Harrington L, Tilley DG, Chen J, Le Corvoisier P, Violin JD, Wei H, Lefkowitz RJ, Rockman HA. Beta-arrestin-mediated beta1-adrenergic receptor transactivation of the egfr confers cardioprotection. *J Clin Invest*. 2007;117:2445-2458.
7. Cherezov V, Rosenbaum DM, Hanson MA, Rasmussen SG, Thian FS, Kobilka TS, Choi HJ, Kuhn P, Weis WI, Kobilka BK, Stevens RC. High-resolution crystal structure of an

engineered human beta2-adrenergic g protein-coupled receptor. *Science*. 2007;318:1258-1265.

8. Preece NE, Nguyen M, Mahata M, Mahata SK, Mahapatra NR, Tsigelny I, O'Connor DT. Conformational preferences and activities of peptides from the catecholamine release-inhibitory (catestatin) region of chromogranin a. *Regul Pept*. 2004;118:75-87.

9. Allu PK, Chirasani VR, Ghosh D, Mani A, Bera AK, Maji SK, Senapati S, Mullasari AS, Mahapatra NR. Naturally occurring variants of the dysglycemic peptide pancreastatin: Differential potencies for multiple cellular functions and structure-function correlation. *J Biol Chem*. 2014;289:4455-4469.

10. Webb B, Sali A. Comparative protein structure modeling using modeller. *Curr Protoc Bioinformatics*. 2014;47:1-5.

11. Hess B, Kutzner C, van der Spoel D, Lindahl E. Gromacs 4: Algorithms for highly efficient, load-balanced, and scalable molecular simulation. *Journal of Chemical Theory and Computation*. 2008;4:435-447.

12. Hornak V, Abel R, Okur A, Strockbine B, Roitberg A, Simmerling C. Comparison of multiple amber force fields and development of improved protein backbone parameters. *Proteins*. 2006;65:712-725.

13. Essmann U, Perera L, Berkowitz ML, Darden T, Lee H, Pedersen LG. A smooth particle mesh ewald method. *The Journal of Chemical Physics*. 1995;103:8577-8593.

14. Ryckaert J-P, Ciccotti G, Berendsen HJC. Numerical integration of the cartesian equations of motion of a system with constraints: Molecular dynamics of n-alkanes. *Journal of Computational Physics*. 1977;23:327-341.

15. Pierce BG, Wiehe K, Hwang H, Kim BH, Vreven T, Weng Z. Zdock server: Interactive docking prediction of protein-protein complexes and symmetric multimers. *Bioinformatics*. 2014;30:1771-1773.

16. Mintseris J, Pierce B, Wiehe K, Anderson R, Chen R, Weng Z. Integrating statistical pair potentials into protein complex prediction. *Proteins*. 2007;69:511-520.

17. Humphrey W, Dalke A, Schulten K. Vmd: Visual molecular dynamics. *J Mol Graph*. 1996;14:33-38.

18. de Beer TA, Berka K, Thornton JM, Laskowski RA. Pdbsum additions. *Nucleic Acids Res*. 2014;42:D292-D296.

19. Laskowski RA, Swindells MB. Ligplot+: Multiple ligand-protein interaction diagrams for drug discovery. *J Chem Inf Model*. 2011;51:2778-2786.

20. Wen G, Mahata SK, Cadman P, Mahata M, Ghosh S, Mahapatra NR, Rao F, Stridsberg M, Smith DW, Mahboubi P, Schork NJ, O'Connor DT, Hamilton BA. Both rare and common polymorphisms contribute functional variation at chga, a regulator of catecholamine physiology. *Am J Hum Genet*. 2004;74:197-207.

21. Choi Y, Miura M, Nakata Y et al. A common genetic variant of the chromogranin a-derived peptide catestatin is associated with atherogenesis and hypertension in a japanese population. *Endocr J*. 2015;62:797-804.

22. Biesecker LG, Mullikin JC, Facio FM et al. The clinseq project: Piloting large-scale genome sequencing for research in genomic medicine. *Genome Res*. 2009;19:1665-1674.

SUPPLEMENTARY TABLES

Supplementary Table S1: Genetic variants identified in the CST domain of *CHGA* in various world populations. *

SNP	rs number	Wild-type base	Variant base	Reference
Y363Y	rs9658666	C	T	Wen *et. al.* 2004[20]
G364S	rs9658667	G	A	Wen *et. al.* 2004[20], Sahu *et. al.* 2012[1]
G367V	rs200576557	G	T	Sahu *et. al.* 2012[1]
P370L	rs9658668	C	T	Wen *et. al.* 2004[20]
R374Q	rs9658669	G	A	Wen *et. al.* 2004[20]

* The naturally-occurring genetic variants discovered in the CST domain of *CHGA* in different world populations are listed along with their rs numbers and the change in nucleotide.

Supplementary Table S2: Clinical characteristics of controls and cases in South Indian populations.*

Parameter	Controls		DM, HTN cases		p value	CAD cases		p value
	N	Mean ± SE	N	Mean ± SE		N	Mean ± SE	
Age (years)	976	39.24 ± 0.348	1702	45.97 ± 0.256	<0.001	514	50.95 ± 0.483	<0.001
Sex (M/F)	976	51.8%/48.2%	1705	58.5%/41.5%		518	87.3%/12.7%	
Height (cm)	600	163.18 ± 0.318	906	162.96 ± 0.281	0.271	338	161.61 ± 0.389	<0.001
Weight (kg)	600	64.59 ± 0.375	902	65.34 ± 0.294	0.488	349	63.05 ± 0.540	0.020
Body Mass Index (kg/m^2)	976	23.75 ± 0.118	1700	24.81 ± 0.091	<0.001		NA	
Heart Rate (beats/minute)	600	77.24 ± 0.334	901	77.19 ± 0.263	1.000	495	79.92 ± 0.570	<0.001
Systolic Blood Pressure (mm Hg)	868	120.03 ± 0.439	1208	142.83 ± 0.545	<0.001	505	127.45 ± 0.887	<0.001
Diastolic Blood Pressure (mm Hg)	868	74.58 ± 0.278	1208	85.66 ± 0.334	<0.001	505	82.15 ± 0.530	<0.001
Mean Arterial Pressure (mm Hg)	868	89.70 ± 0.290	1208	104.77 ± 0.367	<0.001	505	97.26 ± 0.599	<0.001
LVIDd (mm)	600	44.37 ± 0.121	906	44.86 ± 0.117	0.052		NA	
LVIDs (mm)	600	26.73 ± 0.123	906	27.40 ± 0.115	0.001		NA	
Haemoglobin (g/dl)	616	13.36 ± 0.190	1095	13.51 ± 0.114	0.947		NA	
Sodium (meq/l)	562	139.24 ± 0.129	906	136.90 ± 0.172	<0.001	336	135.36 ± 0.516	<0.001
Potassium (meq/l)	562	4.08 ± 0.070	906	4.06 ± 0.044	1.000	339	3.79 ± 0.104	0.028
Urea (mg/dl)	668	20.86 ± 0.269	1397	24.38 ± 0.244	<0.001		NA	
Creatinine (mg/dl)	668	0.81 ± 0.007	1397	0.88 ± 0.005	<0.001		NA	

Random Blood Sugar (mg/dl)	562	96.03 ± 0.687	905	107.78 ± 1.376	<0.001	358	131.85 ± 3.363	<0.001
Total Cholesterol (mg/dl)	937	173.17 ± 1.095	1690	183.77 ± 1.044	<0.001	109	176.28 ± 3.753	0.381
Triglycerides (mg/dl)	937	117.85 ± 1.887	1689	159.22 ± 2.464	<0.001	112	137.92 ± 5.333	<0.001
High Density Lipoproteins (mg/dl)	937	40.41 ± 0.368	1691	40.48 ± 0.268	1.000	76	39.3 ± 0.714	0.297
Low Density Lipoproteins (mg/dl)	937	106.54 ± 0.922	1691	112.61 ± 0.842	<0.001	11	133.45 ± 9.802	0.001
Very Low Density Lipoproteins (mg/dl)	376	23.00 ± 0.631	796	33.96 ± 0.854	<0.001	5	28.52 ± 3.864	0.253
HOMA-IR	363	1.86 ± 0.066	643	4.01 ± 0.126	<0.001		NA	
HbA1c	371	5.58 ± 0.025	794	8.49 ± 0.083	<0.001		NA	
Fasting Blood Sugar (mg/dl)	376	85.11 ± 0.414	796	155.84 ± 2.582	<0.001		NA	
Post Glucose Blood Sugar (mg/dl)	375	99.25 ± 1.057	795	260.85 ± 3.948	<0.001		NA	
FBS Insulin	362	8.84 ± 0.301	643	10.90 ± 0.282	<0.001		NA	
PGBS Insulin	341	56.98 ± 2.403	629	58.14 ± 1.879	0.996		NA	

* Clinical parameters of the overall Chennai population (n=3200) stratified as controls, DM/HTN cases and CAD cases were analysed. Values are shown as mean ± SE. LVIDd: Left ventricular internal diameter at end of diastole, LVIDs: Left ventricular internal diameter at end of systole, HOMA-IR index: Insulin resistance index (Fasting insulin (mIU/L**)** x Fasting glucose (mg/dL**)**/405), HbA1c: glycated haemoglobin, FBS: fasting blood sugar, PGBS: post-glucose blood sugar. NA: Data not available.

Supplementary Table S3: Clinical characteristics of controls and cases in a North Indian population.*

Parameter	Controls		HTN cases		p value
	N	Mean ± SE	N	Mean ± SE	
Age (years)	358	59.77 ± 0.619	377	47.45 ± 0.619	<0.001
Sex (M/F)	358	71.2%/28.8%	377	51.2%/48.8%	
Systolic Blood Pressure (mm Hg)	359	118.48 ± 0.589	388	149.43 ± 0.787	<0.001
Diastolic Blood Pressure (mm Hg)	359	75.69 ± 0.322	388	97.01 ± 0.456	<0.001
Mean Arterial Pressure (mm Hg)	359	89.89 ± 0.312	388	114.49 ± 0.489	<0.001
Total Cholesterol (mg/dl)		NA	349	192.78 ± 2.503	
Triglycerides (mg/dl)		NA	347	173.67 ± 23.719	
High Density Lipoproteins (mg/dl)		NA	339	46.67 ± 0.553	
Low Density Lipoproteins (mg/dl)		NA	344	128.51 ± 1.934	

* Clinical parameters of the overall Chandigarh population (n=760) stratified as HTN cases and controls were analysed. Values are shown as mean ± SE. NA: Data not available.

Supplementary Table S4: Distribution of genotypes and minor allelic frequencies in Indian populations.*

Genotypes	Chennai population		Chandigarh population	
	Cases	Controls	Cases	Controls
GG	1947 (87.5%)	868 (88.9%)	362 (90.3%)	345 (96.1%)
AG	264 (11.9%)	100 (10.2%)	39 (9.7%)	14 (3.9%)
AA	13 (0.6%)	8 (0.8%)	0 (0%)	0 (0%)
Total	2224 (100%)	976 (100%)	401 (100%)	359 (100%)
Minor Allelic Frequency (%)	6.34		3.48	

* The minor allelic frequencies were calculated for the Chennai DM (type-2 diabetes), HTN (hypertension) cases and controls, Chennai CAD (coronary artery disease) cases and Chandigarh HTN cases and controls. There was a drastic difference in the frequencies between the Chennai and Chandigarh populations (χ^2=18.01 and p=0.0001).

Supplementary Table S5: Distribution of genotypes of Gly364Ser SNP in various ethnic/geographical world populations.*

	Population	n	MAF (%)	Reference/Source
Asian	Chinese (Metropolitan Denver, Colorado, USA)	82	7.3	dbSNP / Hapmap Data
	Gujarati Indian (Houston, Texas, USA)	87	6.9	dbSNP / Hapmap Data
	Indian (Chennai, India)	**3200**	**6.3**	**This study**
	Japanese (Ibaraki, Saitama and Shizuoka, Japan)	343	6.1	Choi *et. al.* 2015[21]
	Indian (Chandigarh, India)	**760**	**3.8**	**This study**
	Asian (Southern California, USA)	44	1.8	dbSNP / Wen *et. al.* 2004 [20]
Hispanic	Hispanic (Southern California, USA)	28	5.9	dbSNP / Wen *et. al.* 2004[20]
European	European (Southern California, USA)	52	4.9	dbSNP / Wen *et. al.* 2004[20]
	European (ClinSeq Project)	230	2.4	dbSNP / Biesecker *et. al.* 2009[22]
	Toscan (Italy)	84	2.4	dbSNP / Hapmap Data
African	Luhya (Webuya, Kenya)	87	1.1	dbSNP / Hapmap Data
	Maasai (Kinyawa, Kenya)	142	0.4	dbSNP / Hapmap Data
	African (Southern California, USA)	57	0.0	dbSNP / Wen *et. al.* 2004[20]

*The minor allele frequencies for the Gly364Ser variant in various populations of the world are listed. While the Chennai populations showed minor allele frequencies similar to other Asian populations, the Chandigarh population showed a frequency closer to that displayed by European populations.

SUPPLEMENTARY FIGURES

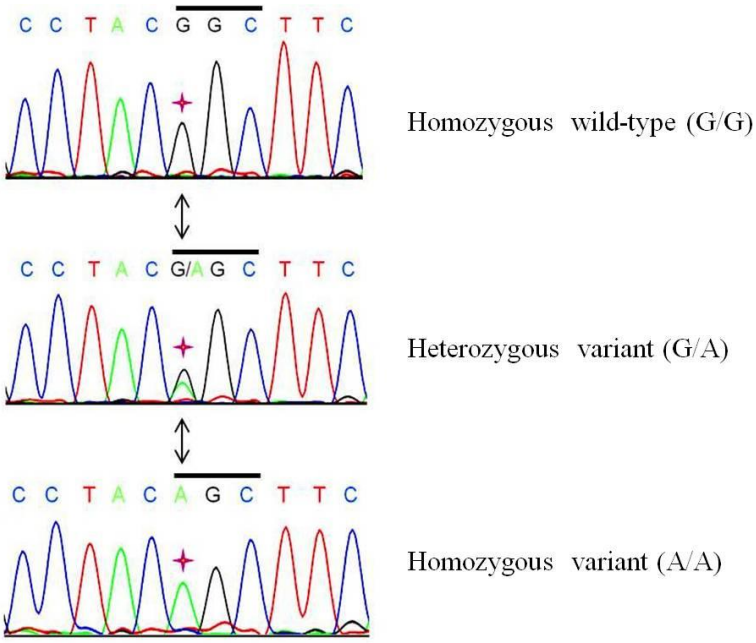

Supplementary Figure S1. Discovery of the naturally-occurring amino acid variant Gly364Ser of catestatin. Resequencing of the catestatin region of the chromogranin A gene was carried out using specific primers. Representative chromatograms for wild-type GG (Gly/Gly), heterozygous variant GA (Gly/Ser) and homozygous variant AA (Ser/Ser) at 9559 bp position are shown. The amino acid number indicated, i.e., 364, is with respect to the mature chromogranin A protein, which is equivalent to the 382nd amino acid in the pre-protein that includes the 18 aa long signal peptide. Here, the 1st nucleotide (indicated by *) of the codon GGC (in the wild-type) is altered to AGC (in the variant) changing the amino acid Gly to Ser.

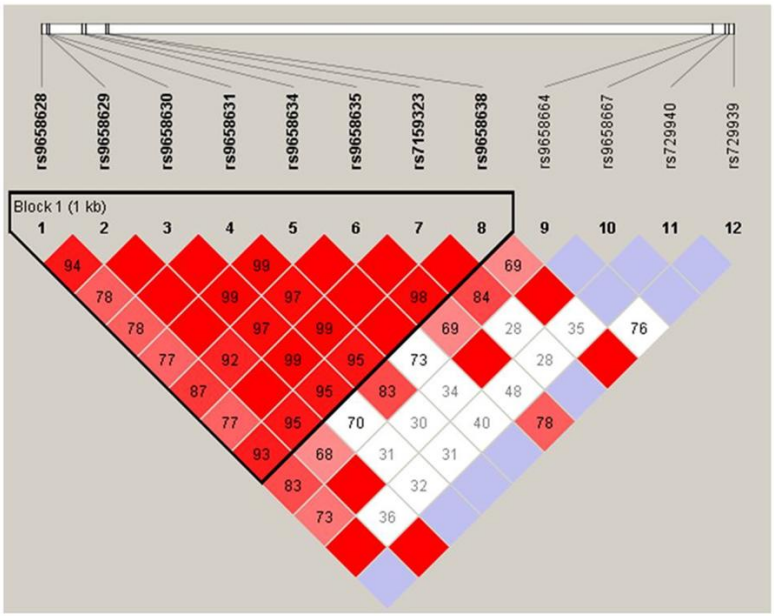

L1	Position	L2	Position	D'	CI	LOD	r^2
rs9658667	Exon 7 (G364S)	rs9658628	Promoter (-1106)	0.734	0.63-0.82	29.63	0.245
rs9658667	Exon 7 (G364S)	rs9658629	Promoter (-1018)	1	0.62-1.00	4.10	0.023
rs9658667	Exon 7 (G364S)	rs9658635	Promoter (-415)	1	0.80-1.00	8.49	0.043
rs9658667	Exon 7 (G364S)	rs9658638	Promoter (-57)	1	0.58-1.00	3.71	0.022
rs9658667	Exon 7 (G364S)	rs9658664	Exon 7 (G297S)	1	0.27-1.00	1.51	0.006
rs9658667	Exon 7 (G364S)	rs729940	Exon 7 (R381W)	1	0.36-1.00	1.94	0.007
rs9658667	Exon 7 (G364S)	rs729939	Exon 7 (E403E)	1	0.21-1.00	1.24	0.006

Supplementary Figure S2. Linkage disequilibrium (LD) among CST Gly364Ser and other *CHGA* variants.

LD pattern of 12 common biallelic polymorphisms discovered in the *CHGA* promoter and exon-7 region of 581 individuals. Pairwise results are plotted on a pseudocolor scale for LD with Haploview. Bright red represents D'=1, LOD≥2; blue represents D'=1, LOD<2; shades of pink/red represent D'<1, LOD≥2; white represents D'<1, LOD<2. Number in diamond shape represents LD as D'×100. LD blocks are determined by the four-gamete rule.

LOD: logarithm of odds.

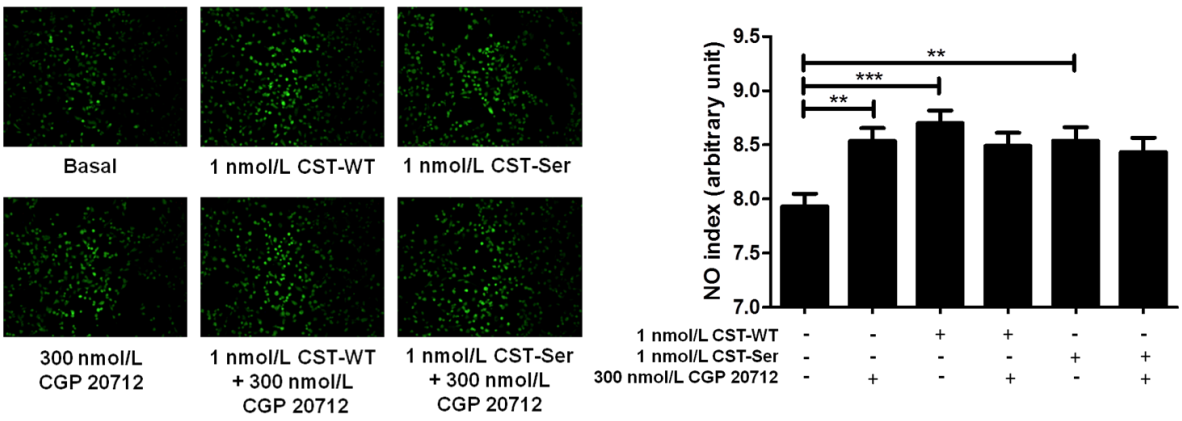

Supplementary Figure S3. Effect of ADRB1 antagonist CGP 20712 on NO production in HUVECs treated with CST peptides.

The fluorescence intensities (NO indices) were calculated by Image J analysis and plotted as mean ± SE. The experimental groups were compared by one-way ANOVA followed by Tukey's multiple comparison post-test. Representative images for the treatment of HUVECs with 300 nmol/L CGP 20712, 1 nmol/L CST-WT, 1 nmol/L CST-364Ser, 1 nmol/L CST-WT + 300 nmol/L CGP 20712, 1 nmol/L CST-364Ser + 300 nmol/L CGP 20712. *** represents $p<0.001$ for basal vs. CST-WT peptide, ** represents $p<0.01$ for basal vs. CGP 20712, basal vs. CST-364Ser. Overall one-way ANOVA $F=4.727$, $p=0.0003$; n=450 cells/condition.

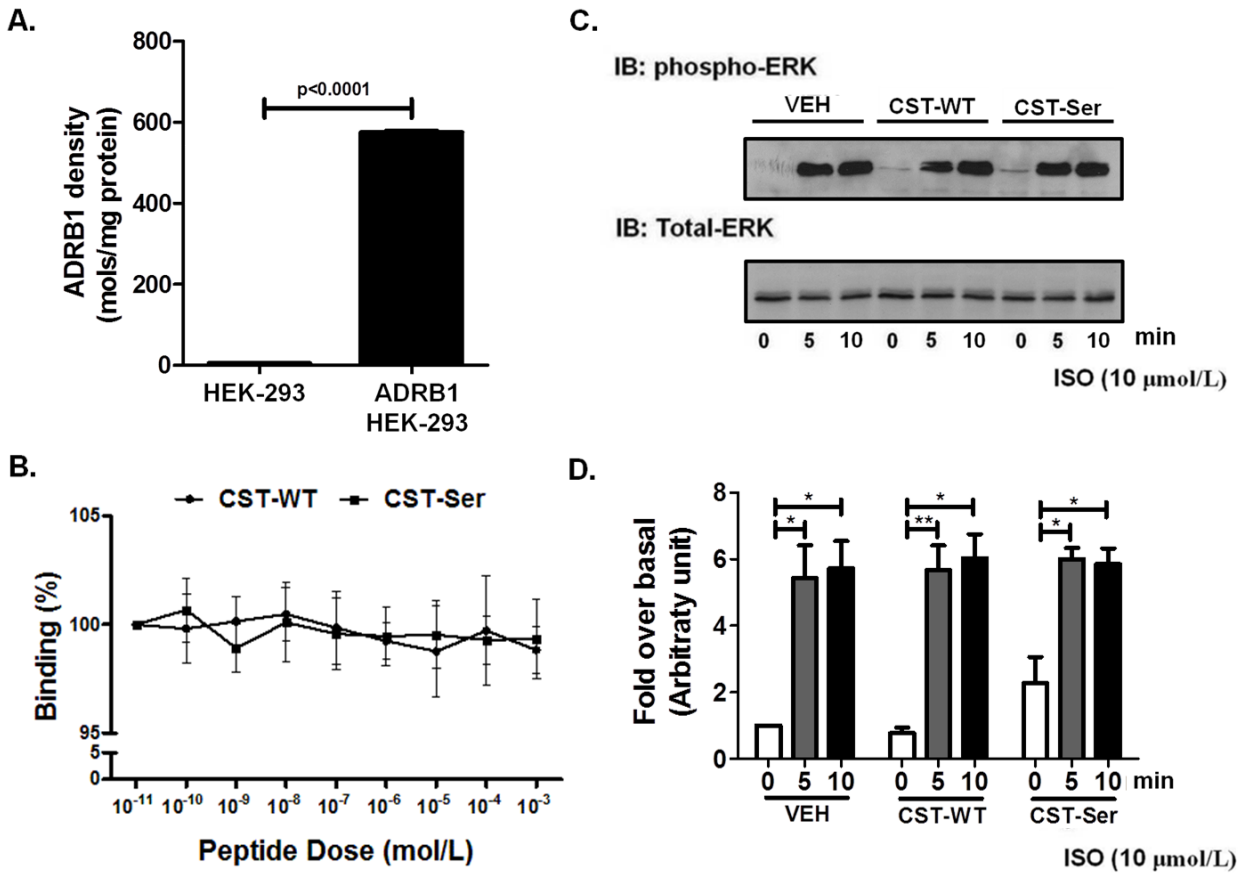

Supplementary Figure S4. Binding of CST peptides to ADRB1 receptor and downstream effects.

Panel A: ADRB1 HEK-293 cells showed ~109-fold higher expression of ADRB1 ($p<0.0001$) as compared to control HEK-293 cells. Data are shown as ADRB1 levels normalized with total protein.

Panel B: Data are shown as percentage binding of the radio-ligand cyanopindolol. With increasing doses of CST-WT and CST-364Ser (10 pmol/L to 1 mmol/L), there was no displacement of the ligand. The experimental groups were compared by one-way ANOVA followed by Tukey's multiple comparison post-test.

Panels C and D: Representative western blot (panel C) and quantitative representation of the densitometric analysis from 4 independent experiments (panel D) showing phosphorylated ERK (pERK) and total ERK levels upon treatment with CST peptides and isoproterenol

(ISO). ISO (10 μmol/L) showed an increase in pERK levels at 5 min and 10 min in the vehicle (VEH) condition, reflecting the activation of ADRB1. However, this increase remain unaffected upon pre-treatment with both CST-WT (10 μmol/L) and CST-364Ser (10 μmol/L). The experimental groups were compared by t-test.

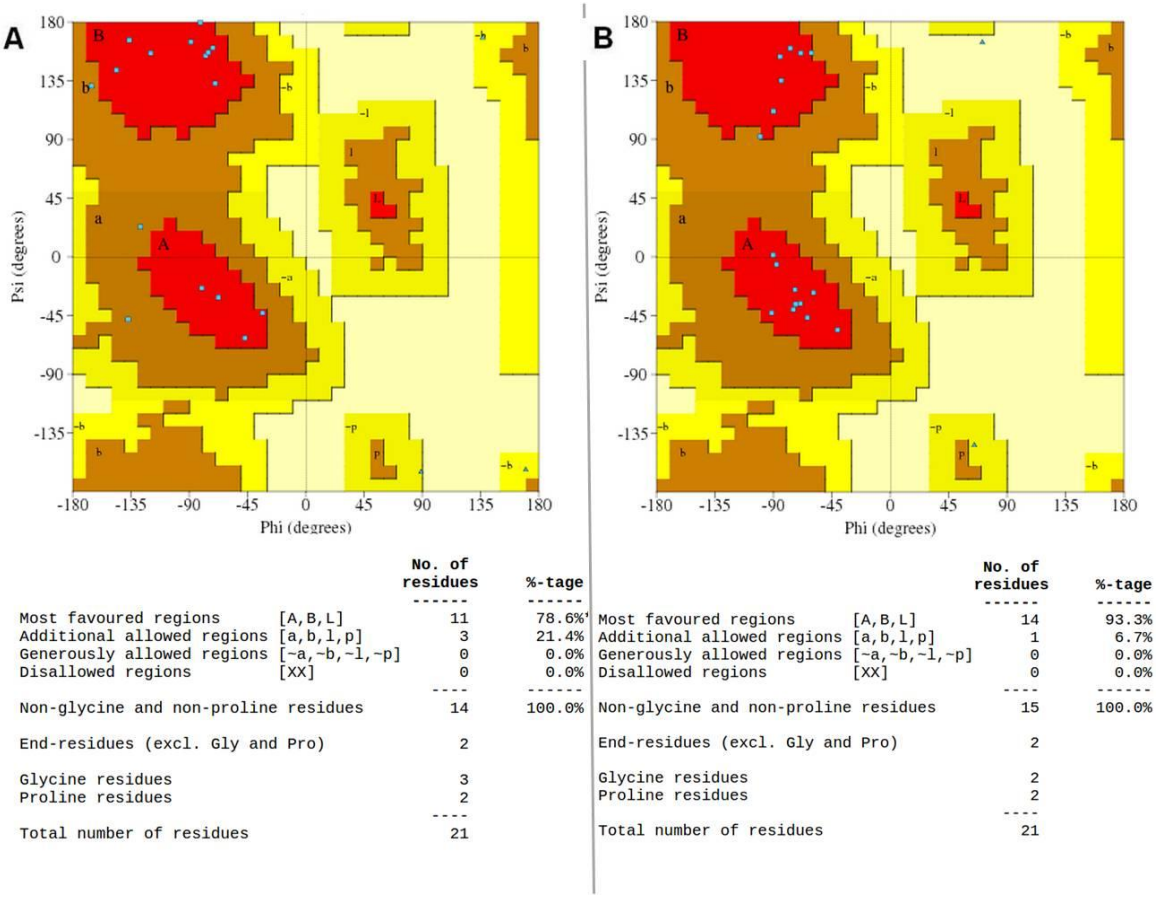

		No. of residues	%-tage
Most favoured regions	[A,B,L]	11	78.6%
Additional allowed regions	[a,b,l,p]	3	21.4%
Generously allowed regions	[~a,~b,~l,~p]	0	0.0%
Disallowed regions	[XX]	0	0.0%
Non-glycine and non-proline residues		14	100.0%
End-residues (excl. Gly and Pro)		2	
Glycine residues		3	
Proline residues		2	
Total number of residues		21	

		No. of residues	%-tage
Most favoured regions	[A,B,L]	14	93.3%
Additional allowed regions	[a,b,l,p]	1	6.7%
Generously allowed regions	[~a,~b,~l,~p]	0	0.0%
Disallowed regions	[XX]	0	0.0%
Non-glycine and non-proline residues		15	100.0%
End-residues (excl. Gly and Pro)		2	
Glycine residues		2	
Proline residues		2	
Total number of residues		21	

Supplementary Figure S5. Ramachandran plots for the modelled structures of CST-WT and CST-364Ser peptides. Panel A and Panel B are the Ramachandran plots for CST-WT and CST-364Ser, respectively. In both the panels, the yellow, brown and red colored areas represent generously allowed, additionally allowed and most favoured regions, respectively. Amino acid residues falling in the allowed region are represented by blue dots. Regions A, B and L correspond to the residues involved in the formation of right handed alpha-helices, beta-sheets and left handed alpha-helices, respectively.

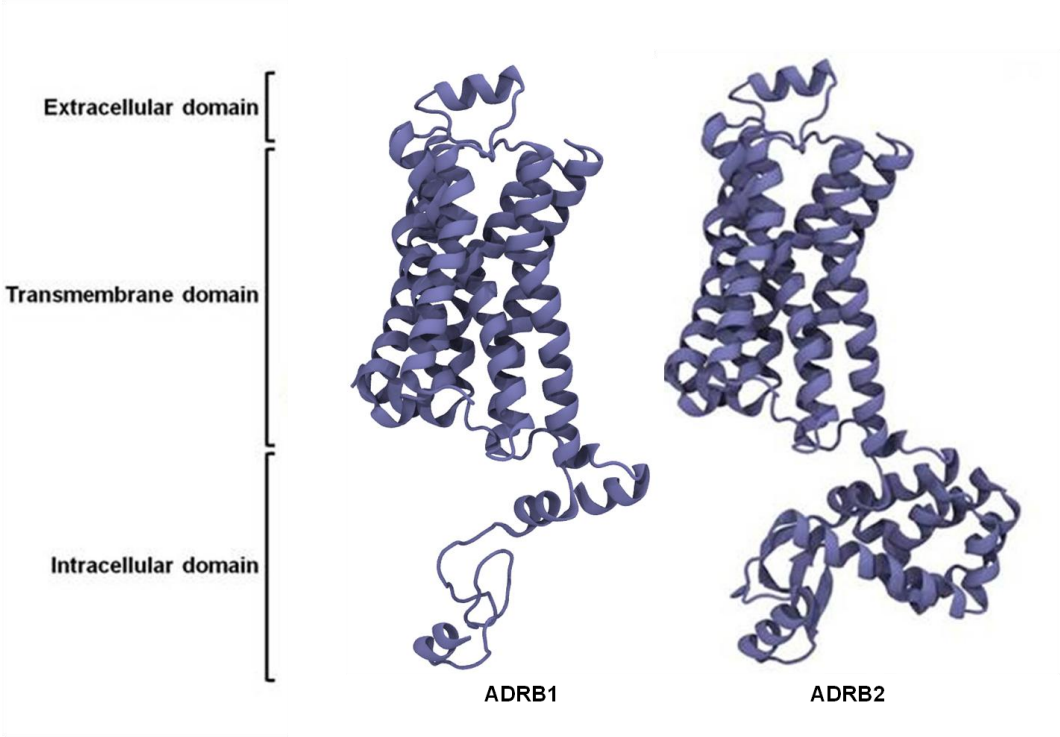

Supplementary Figure S6. Modelled structure of human beta1- and beta2-adrenergic receptor (ADRB1/2). The figure shows the 3-dimensional conformation of ADRB1 (left) and ADRB2 (right) in cartoon representation. The structure of ADRB2 is based on the crystal structure of ADRB2 with resolution 2.4 Å obtained from protein data bank (PDB ID:2RH1). The bound ligands and the crystal water were stripped from the protein crystal structure and subsequently energy minimized to obtain the above sophisticated model of ADRB2 for protein-protein docking. The structure of ADRB1 was modelled based on the template of ADRB2. The extracellular domain, the transmembrane domain and the intracellular domain have been labelled.

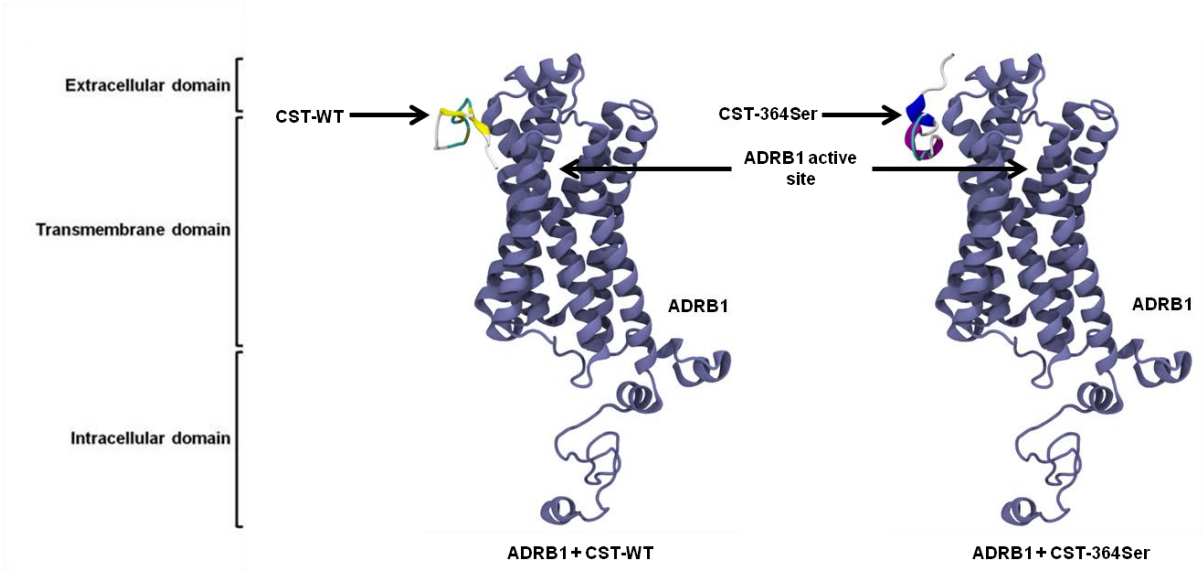

Supplementary Figure S7. Interactions of CST peptides with ADRB1. The figure shows the docking of CST-WT (left) and CST-364Ser (right) to ADRB1. ADRB1 is colored violet, the beta-sheet in CST-WT is shown in yellow, while the alpha-helix and 3_{10}-helix in CST-364Ser are shown in purple and blue respectively.

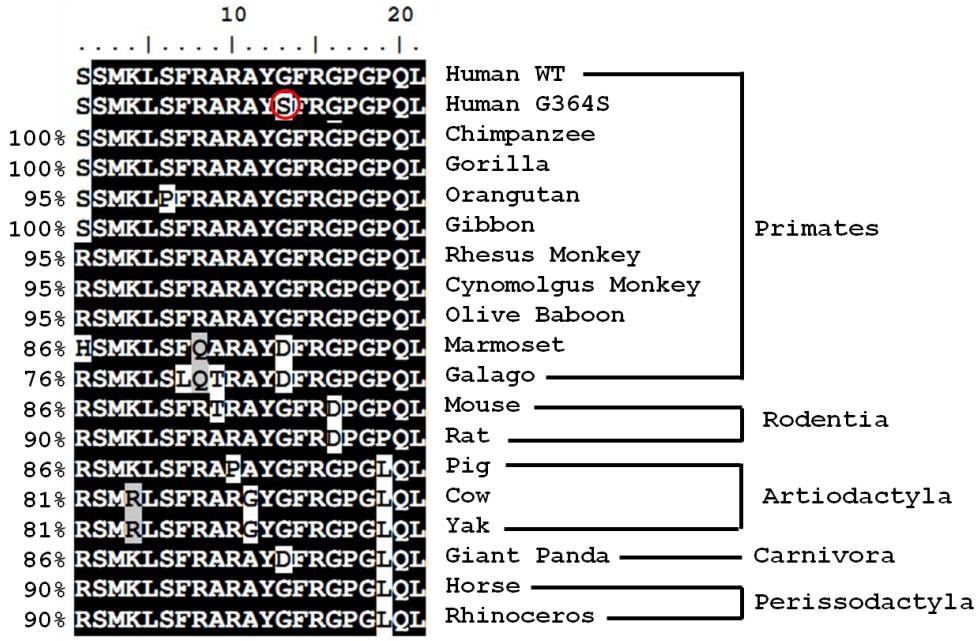

Supplementary Figure S8. Human CST variants and inter-species homology among Eutherian mammals. ClustalW multiple sequences alignment was carried out using BioEdit version 7.2.5 (Ibis Biosciences, Carlsbad, CA, USA); the percentages of homology are given on the left side. These organisms are arranged according to their Order. Human variant is encircled in red. The identical amino acid residues from all species are shaded with dark grey color and similar amino acid residues are shaded with light grey color. All the species showed a minimum of 76% similarity in CST region of *CHGA*. CST sequences used are - Primates: Human (accession number NM_001275), Common chimpanzee (XP_510135.3), Gorilla (XP_004055643.1), Sumatran orang-utan (XP_002825091.1), White-cheeked gibbon (XP_003260951.1), Rhesus monkey (XP_001092629.2), Cynomolgus monkey (BAE01874.1), Olive baboon (XP_003902238.1), Marmoset (XP_002754260.1) and Galago (XP_003787045.1), Rodentia: House mouse (NP_031719.1) and Common rat (AEB41037.1), Artiodactyla: Wild pig (NP_001157477.2), Cow (NP_851348.1) and Yak (ELR47684.1), Carnivora: Giant panda (XP_002923879.1), Perissodactyla: Horse (NP_001075283.1) and White rhinoceros (XP_004434274.1)

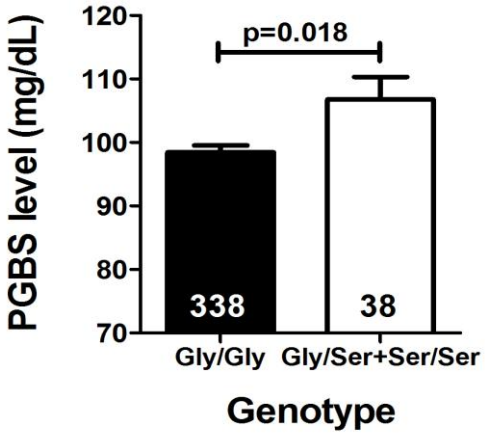

Supplementary Figure S9. **Allele-specific associations of human post-glucose blood sugar levels *in vivo.*** In the Chennai controls population, subjects were stratified into Gly/Gly and Gly/Ser+Ser/Ser groups. The post-glucose blood sugar levels, measured by standard biochemical assays, were compared between the two groups. Data are shown as mean ± SE. Statistical significance between the groups was determined by Levene's test for equality of variances and t-test for equality of means using SPSS software (SPSS Inc., Chicago, IL). The PGBS levels in 364Ser carrying individuals were elevated than wild-type individuals in this population.